7918 J. Med. Chem. 2010, 53, 7918–7931
DOI: 10.1021/jm100286k

Journal of Medicinal Chemistry Article

4-Oxo-1,4-dihydropyridines as Selective CB_2 Cannabinoid Receptor Ligands: Structural Insights into the Design of a Novel Inverse Agonist Series

Jamal El Bakali,[†,⊥] Giulio G. Muccioli,[‡,#,⊥] Nicolas Renault,[§] Delphine Pradal,[†] Mathilde Body-Malapel,[∥] Madjid Djouina,[∥] Laurie Hamtiaux,[‡] Virginie Andrzejak,[†] Pierre Desreumaux,[∥] Philippe Chavatte,[§] Didier M. Lambert,*[,‡] and Régis Millet*[,†]

[†]*Université Lille-Nord de France, Institut de Chimie Pharmaceutique Albert Lespagnol, EA 2692, IFR 114, 3 Rue du Professeur Laguesse, BP 83, 59006 Lille Cedex, France,* [‡]*Unité de Chimie Pharmaceutique et de Radiopharmacie, Louvain Drug Research Institute, Université Catholique de Louvain, 73 Avenue E. Mounier UCL-CMFA (7340), B-1200 Bruxelles, Belgium,* [§]*Université Lille-Nord de France, Faculté de Pharmacie, Laboratoire de Chimie Thérapeutique, EA 1643, IFR 114, 3 Rue du Professeur Laguesse, BP 83, 59006 Lille Cedex, France, and* [∥]*Physiopathologie des Maladies Inflammatoires de l'Intestin, Université Lille-Nord de France, Amphi J & K, U795, IFR 114, Boulevard du Professeur Leclercq, 59045 Lille Cedex, France.* [⊥]*Both authors contributed equally to this work.*
[#]*Present address: Bioanalysis and Pharmacology of Bioactive Lipids Lab, Louvain Drug Research Institute, Université Catholique de Louvain, 72 Avenue E. Mounier UCL-CHAM (7230), B-1200 Bruxelles, Belgium*

Received March 4, 2010

Growing evidence shows that CB_2 receptor is an attractive therapeutic target. Starting from a series of 4-oxo-1,4-dihydroquinoline-3-carboxamide as selective CB_2 agonists, we describe here the medicinal chemistry approach leading to the development of CB_2 receptor inverse agonists with a 4-oxo-1,4-dihydropyridine scaffold. The compounds reported here show high affinity and potency at the CB_2 receptor while showing only modest affinity for the centrally expressed CB_1 cannabinoid receptor. Further, we found that the functionality of this series is controlled by its C-6 substituent because agonists bear a methyl or a *tert*-butyl group and inverse agonists, a phenyl or 4-chlorophenyl group, respectively. Finally, in silico studies suggest that the C-6 substituent could modulate the conformation of W6.48 known to be critical in GPCR activation.

Introduction

The CB_2 receptor belongs to the class A of G protein-coupled receptors superfamily. It is one of the components of the endocannabinoid system, which is a physiological system composed of cannabinoid receptors, CB_1 and CB_2, their endogenous ligands, named endocannabinoids, and the biotransformation enzymes involved in the synthesis, degradation, and cellular uptake of these endocannabinoids.[1−3] This system plays a key role in numerous biological processes and is involved in maintaining homeostasis. Cannabinoids exhibit pharmacological effects in a large spectrum of diseases and disorders.[4] Thus, in the past years, investigations were aimed at designing new synthetic molecules that target cannabinoid receptors. One of the main challenges for such compounds is to be as much as possible devoid of central nervous system (CNS[a]) side effects. Because these undesirable effects are thought to be CB_1 receptor-mediated,[5] the main strategy to avoid them is to develop CB_2 selective ligands.[6] The high expression of CB_2 receptor in immune tissues and cells, both in periphery[2,7] and in the CNS[8,9] as well as the enhancement of its expression following inflammatory insults,[10,11] suggests that CB_2 receptor selective ligands might be effective in modulating inflammation. These observations were confirmed by the lack of immunomodulation induced by cannabinoids in CB_2 knockout mice.[12] The CB_2 receptor exerts a critical role in the immune system by modulating cytokines release[13,14] and immune cells migration.[15−17] Besides, recent studies have emphasized the major role of CB_2 receptors in pathologies where an inflammatory component is involved, including Alzheimer disease,[18] inflammatory bowel disease,[19−21] or multiple sclerosis.[22,23] Other studies indicate that CB_2 receptors could be involved in alleviating pain[24] and could provide protection from bone loss.[25]

This therapeutic potential has prompted the development of several CB_2 receptor selective ligands, either as agonists or as antagonists/inverse agonists (Chart 1). Among the selective agonists, classical cannabinoids and aminoalkylindoles have been extensively studied.[26−28] (6a*R*,10a*R*)-3-(1,1-Dimethylbutyl)-6a,7,10,10a-tetrahydro-6,6,9-trimethyl-6*H*-dibenzo[*b*,*d*]pyran (**1**, JWH-133) was shown to decrease experimental colitis induced by oil of mustard and dextran sulfate sodium in vivo,[19] whereas (1-(2-morpholin-4-yl-ethyl)-1*H*-indol-3-yl)-(2,2,3,3-tetramethylcyclopropyl) methanone (**2**, A-796260) has demonstrated analgesic activity in models of inflammatory, postoperative, neuropathic, and osteoarthritic pain.[24] More

*To whom correspondence should be addressed. For R.M.: phone, +33-3-2096-4374; fax, +33-3-2096-4906; E-mail, régis.millet@univ-lille2.fr. For D.M.L.: phone, +32-2-764-7347; fax, +32-2-764-7363; E-mail, didier.lambert@uclouvain.be.

[a] Abbreviations: CNS, central nervous system; CHO, Chinese hamster ovary; *h*CB_1, human CB_1 cannabinoid receptor; *h*CB_2, human CB_2 cannabinoid receptor; K_i, inhibition constant; EC_{50}, half-maximal effective concentration; [^{35}S]-GTPγS, guanosine-5′-*O*-(3-[^{35}S]thio)-triphosphate); E_{max}, maximum efficacy; TM, transmembrane domain; EL, extracellular loop; rmsd, root-mean-square deviation; LHMDS, lithium hexamethyldisilazane; DMF, *N*,*N*-dimethylformamide; DMS, dimethylsulfate; EtOAc, ethyl acetate; EtOH, ethanol; AcOH, acetic acid; DMSO, dimethylsulfoxide; DIPEA, *N*,*N*-diisopropylethylamine; HOBt, 1-hydroxybenzotriazole; HBTU, 2-(1*H*-benzotriazol-1-yl)-1,1,3,3-tetramethyluronium hexafluorophosphate; DPPA, diphenylphosphoryl azide; *t*-BuOK, potassium *tert*-butoxide; *t*-BuOH, *tert*-butyl alcohol; rt, room temperature; TLC, thick-layer chromatography

 Published on Web 10/27/2010

Chart 1. Structure of Representatives CB_2 Selective Ligands (**1**) JWH-133, (**2**) A-796260, (**3**) CBS-0550, (**4**) GW842166X, (**5**) SR144528, (**6**) JTE907, (**7**) Sch225336, (**8**) ALICB122

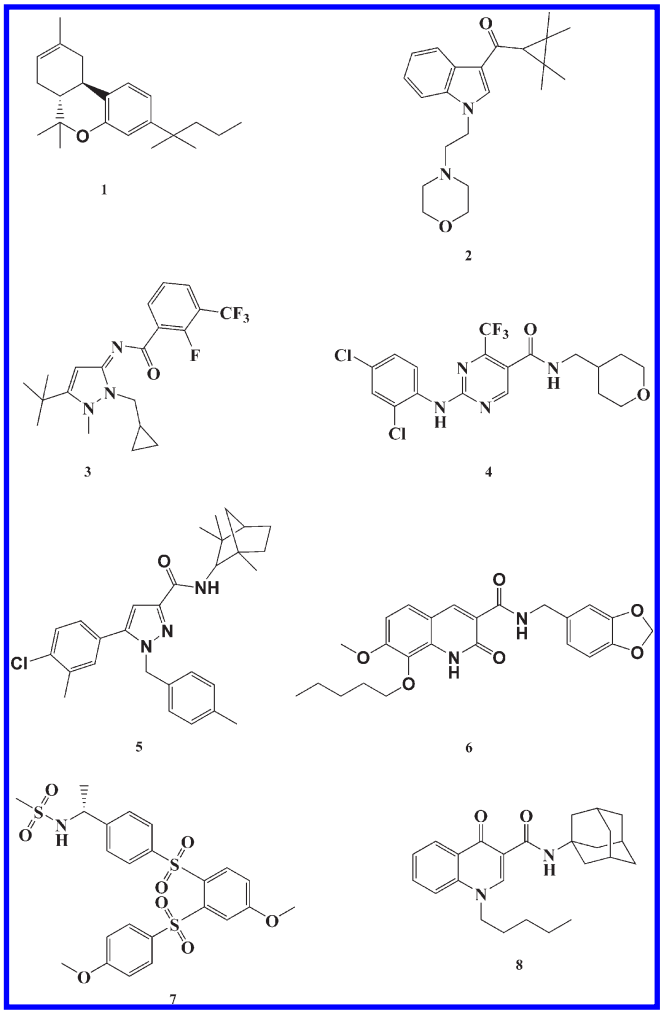

recently, other compounds have been disclosed such as the iminopyrazole *N*-(5-*tert*-butyl-2-cyclopropylmethyl-1-methyl-1,2-dihydropyrazol-3-ylidene)-2-fluoro-3-(trifluoromethyl)-benzamide (**3**, CBS-0550)[29] and the pyrimidine derivative 2-[(2,4-dichlorophenyl)amino]-*N*-[(tetrahydro-2*H*-pyran-4-yl)-methyl]-4-(trifluoromethyl)-5-pyrimidinecarboxamide (**4**, GW842166X),[30] which was chosen as a clinical candidate for the treatment of inflammatory pain. As for selective antagonists/inverse agonists, much fewer compounds have been described. The first to be discovered and the most widely used is the 1,5-diarylpyrazole, 5-(4-chloro-3-methylphenyl)-1-[(4-methylphenyl)methyl]-*N*-[(1*S*,4*R*,6*S*)-1,5,5-trimethyl-6-bicyclo[2.2.1]-heptanyl]pyrazole-3-carboxamide (**5**, SR144528).[31] This compound as well as the 2-quinolone derivative *N*-(benzo[1,3]-dioxol-5-ylmethyl)-7-methoxy-2-oxo-8-pentyloxy-1,2-dihydroquinoline-3-carboxamide (**6**, JTE907) received attention due to their anti-inflammatory properties.[32] More recently, a new class of CB_2 selective inverse agonists based on a triaryl bissulfone scaffold has been described.[33−35] This class is represented by *N*-[1(*S*)-[4-[[4-methoxy-2-[(4-methoxyphenyl)sulfonyl]phenyl]-sulfonyl]phenyl]ethyl]methanesulfonamide (**7**, Sch225336), which was shown to block the recruitment of leucocytes in vivo.[36] Taken together, the available data strongly support CB_2 ligands as modulators of inflammation.

Chart 2. General Structure of the Tested Compounds **11**, **17**−**41**, and **43**

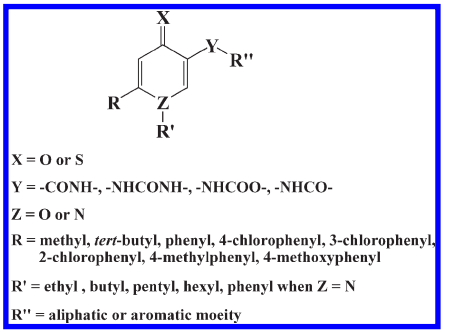

However, it is essential to better understand the pharmacology of CB_2 receptor ligands because, for instance, anti-inflammatory properties have been described for both agonists and inverse agonists. Similar trends were observed concerning studies on bone physiology. Indeed, some authors suggested that blocking the CB_2 receptor protects from bone loss in ovariectomized mice[37,38] and others showed the same effect using the highly selective CB_2 receptor agonist {4-[4-(1,1-dimethylheptyl)-2,6-dimethoxy-phenyl]-6,6-dimethyl-bicyclo[3.1.1]hept-2-en-2-yl}-methanol (HU-308, structure not shown).[25,39]

In this context, our groups previously described the synthesis, pharmacological characterization, and structure−activity relationships of selective CB_2 ligands based on a 4-oxo-1,4-dihydroquinoline-3-carboxamide scaffold (e.g., **8**).[40,41] The structure−activity relationship studies highlighted a significant correlation between affinity and/or selectivity toward the CB_2 receptor and structural features such as an aliphatic moiety, especially an adamantyl substituent, on the C-3 carboxamide group as well as a *n*-pentyl chain in *N*-1 position. Concerning the functionality of these ligands, most of the compounds behaved as selective CB_2 agonists and, more surprisingly, small changes in the position of the substituents around the heterocycle resulted in modifications of the compounds functionality.[41]

In light of these considerations, we sought to find new CB_2 selective ligands. Our efforts to identify such compounds allowed us to describe novel series of 4-oxo-1,4-dihydropyridines and 4-thioxo-1,4-dihydropyridines (general structure shown in Chart 2) that were found to be potent and selective CB_2 receptor ligands. We also report here the identification of a key substituent on the 4-oxo-1,4-dihydropyridine scaffold responsible for a functionality switch within this series of compounds.

Chemistry

The synthesis of *N*3-(1-adamantyl)-6-methyl-1-pentyl-4-oxo-1,4-dihydropyridine-3-carboxamide (compound **11**), outlined in Scheme 1, was performed using a methodology adapted from the literature.[42,43] The commercially available 4-hydroxy-6-methyl-2-pyrone was reacted with *N*,*N*-dimethylformamide dimethyl acetal in mild conditions to give **9**, which, when treated with *n*-pentylamine under alkaline conditions followed by acidification gave the carboxylic acid **10**. Finally, amidation was accomplished with 1-aminoadamantane hydrochloride under peptide coupling conditions to give the target amide **11**.

The synthesis of the 6-*tert*-butyl, 6-phenyl or 6-(4-chlorophenyl) substituted 4-oxo-1,4-dihydropyridine-3-carboxamides and 4-thioxo-1,4-dihydropyridine-3-carboxamides **17**−**36** is

Scheme 1[a]

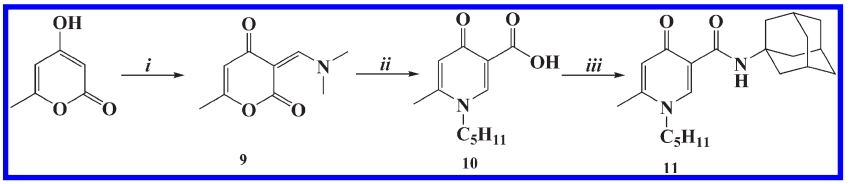

[a] Reagents and conditions: (i) DMF-DMA, dioxane, rt, 4 h, 63%; (ii) *t*-BuOK, *n*-pentylamine, EtOH, reflux, 12 h, 73%; (iii) (a) HOBt, HBTU, DIPEA, DMF, rt, 3 h, (b) 1-aminoadamantane hydrochloride, rt, 12 h, 57%.

Scheme 2[a]

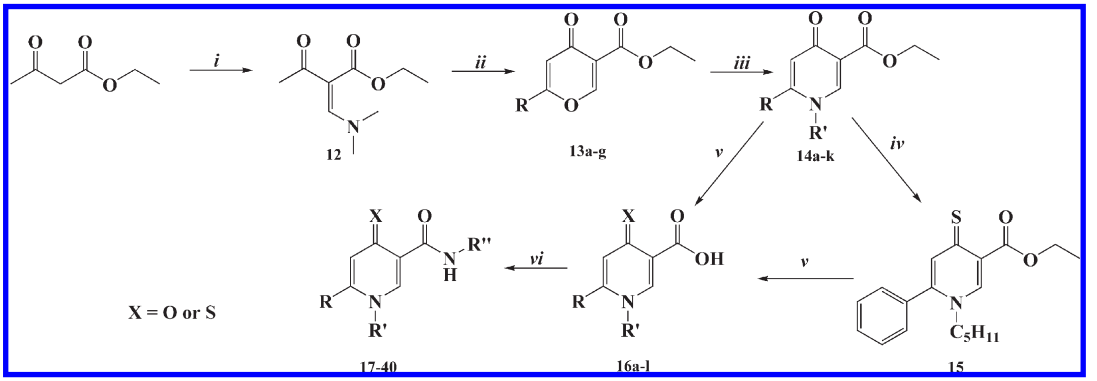

[a] Reagents and conditions: (i) DMF/DMS, Et_3N, CH_2Cl_2, rt, 2 h, 79%; (ii) (a) LHMDS, RCOCl, THF, −78 °C, 15 min, (b) 3N HCl, Et_2O, rt, 45 min, 35−67%; (iii) R′-NH_2, AcOH/EtOH 1:3 reflux, 1−4 h, 45−77%; (iv) (when **14d**) P_4S_{10}, pyridine, reflux, 12 h, 90%; (v) 10% NaOH/EtOH v/v, reflux, 6 h, 66−96%; (vi) (a) HOBt, HBTU, DIPEA, DMF, rt, 3 h, (b) R″-NH_2, rt, 12 h, 28−74%.

described in Scheme 2. Structures of intermediate compounds **13**−**16** as well as target amides **17**−**40** are summarized in Table 1. The 4-oxo-1,4-dihydropyridine scaffold was prepared from ethyl acetoacetate as previously described.[44] Enaminone **12** was obtained by reaction of ethyl acetoacetate with the *N*, *N*-dimethylformamide/dimethylsulfate adduct (DMF/DMS) in combination with triethylamine. Subsequent deprotonation of **12** with lithium hexamethyldisilazane (LHMDS) in the presence of the appropriate acyl chloride at −70 °C followed by acidification at room temperature led directly to pyran-4-ones **13a**−**g**. Aminolysis in acidic conditions afforded 4-oxo-1,4-dihydropyridines **14a**−**k** in acceptable yields. The analogue 4-thioxo-1,4-dihydropyridine **15** was synthesized in very good yields from the corresponding 4-oxo-1,4-dihydropyridine (**14d**) by a thionation reaction using phosphorus pentasulfide as reagent. After saponification of the ethyl ester functions of compounds **14a**−**k** and **15** (sodium hydroxide), the resulting carboxylic acids **16a**−**l** were engaged in an amidation reaction with the appropriate amines under peptide coupling conditions to afford target amide compounds **17**−**40**. Carboxylic acid **16d** was also converted to the carbamate **41** (Boc protected amine) via a Curtius rearrangement using diphenylphosphoryl azide and potassium *tert*-butoxide as reagents and *tert*-butanol as solvent (Scheme 3). Treatment of **41** with hydrochloric acid in isopropyl alcohol followed by neutralization led to amine **42**. The latter reacted with cyclohexyl carboxylic acid under peptide coupling conditions to afford the "reverse amide" **43**.

Pharmacology

The affinities of the newly synthesized compounds **11**, **17**−**41**, and **43** were determined by a competitive radioligand displacement assay using [^{3}H]-CP55,940 and [^{3}H]-SR141716A as radioligands for human CB_2 cannabinoid receptor ($h$$CB_2$) and human CB_1 cannabinoid receptor ($h$$CB_1$), respectively, as previously described.[45] Membranes from Chinese hamster ovary (CHO) cells expressing either the $h$$CB_1$ or the $h$$CB_2$ cannabinoid receptor were used in these experiments. All compounds were first screened at 10 μM concentration for their affinity toward both cannabinoid receptors. The inhibition constant (K_i) values were then determined for compounds exhibiting a specific displacement superior to 60% either for $h$$CB_1$ or the $h$$CB_2$ (Table 2), and the selectivity index (CB_2 vs CB_1) was calculated whenever possible. We also investigated their functionality at the CB_2 receptor using a guanosine-5′-*O*-(3-[^{35}S]thio)triphosphate ([^{35}S]-GTPγS) binding assay and $h$$CB_2$−CHO cells membranes, as previously described.[46] This assay constitutes a functional measure of the interaction of the receptor and the G-protein, the first step in activation of the G-protein coupled receptors. In this system, neutral antagonists do not affect [^{35}S]-GTPγS binding, while agonists and inverse agonists respectively increase and decrease nucleotide binding. The functionality of reference cannabinoid agonists **1**, WIN-55,212-2 and CP-55,940 as well as the inverse agonist **5** were determined. Half-maximal effective concentration (EC_{50}) and maximum efficacy (E_{max}) values of reference and original compounds are summarized in Table 3.

Structure−Affinity/Activity Relationships

The starting point of our investigation was the lead compound **8**, which was described by our groups as a potent selective CB_2 agonist (K_i = 16.4 nM). In the present work, we removed the condensed benzene ring of 4-oxo-1,4-dihydroquinoline-3-carboxamide derivatives resulting in the 4-oxo-1,4-dihydropyridine core. A set of four compounds was first synthesized on the basis of our previously reported work (**11**, **17**, **25**, and **32**).[40] These compounds possessed some features in common, like the *N*-1 pentyl chain and a carboxamidoadamantyl

Table 1. Structures of the Newly Synthesized Compounds **13**−**40**

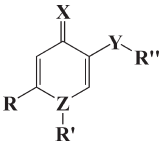

compd	R	R′	R″	X	Y	Z
13a	*tert*-butyl			O	COOEt	O
13b	phenyl			O	COOEt	O
13c	4-chlorophenyl			O	COOEt	O
13d	3-chlorophenyl			O	COOEt	O
13e	2-chlorophenyl			O	COOEt	O
13f	4-methylphenyl			O	COOEt	O
13g	4-methoxyphenyl			O	COOEt	O
14a	*tert*-butyl	pentyl		O	COOEt	N
14b	phenyl	ethyl		O	COOEt	N
14c	phenyl	butyl		O	COOEt	N
14d	phenyl	pentyl		O	COOEt	N
14e	phenyl	hexyl		O	COOEt	N
14f	phenyl	phenyl		O	COOEt	N
14g	4-chlorophenyl	pentyl		O	COOEt	N
14h	3-chlorophenyl	pentyl		O	COOEt	N
14i	2-chlorophenyl	pentyl		O	COOEt	N
14j	4-methylphenyl	pentyl		O	COOEt	N
14k	4-methoxyphenyl	pentyl		O	COOEt	N
15	phenyl	pentyl		S	COOEt	N
16a	*tert*-butyl	pentyl		O	COOH	N
16b	phenyl	ethyl		O	COOH	N
16c	phenyl	butyl		O	COOH	N
16d	phenyl	pentyl		O	COOH	N
16e	phenyl	hexyl		O	COOH	N
16f	phenyl	phenyl		O	COOH	N
16g	4-chlorophenyl	pentyl		O	COOH	N
16h	3-chlorophenyl	pentyl		O	COOH	N
16i	2-chlorophenyl	pentyl		O	COOH	N
16j	4-methylphenyl	pentyl		O	COOH	N
16k	4-methoxyphenyl	pentyl		O	COOH	N
16l	phenyl	pentyl		S	COOH	N
17	*tert*-butyl	pentyl	1-adamantyl	O	CONH	N
18	*tert*-butyl	pentyl	cyclohexyl	O	CONH	N
19	phenyl	ethyl	(*R*,*S*)-1-(adamantyl)ethyl	O	CONH	N
20	phenyl	pentyl	(*R*,*S*)-1-(adamantyl)ethyl	O	CONH	N
21	phenyl	phenyl	(*R*,*S*)-1-(adamantyl)ethyl	O	CONH	N
22	phenyl	pentyl	1-(adamantyl)methyl	O	CONH	N
23	phenyl	pentyl	1-(3,5-dimethyl)adamantyl	O	CONH	N
24	phenyl	butyl	1-adamantyl	O	CONH	N
25	phenyl	pentyl	1-adamantyl	O	CONH	N
26	phenyl	hexyl	1-adamantyl	O	CONH	N
27	phenyl	pentyl	cyclohexyl	O	CONH	N
28	phenyl	pentyl	(*R*)-1-(1,2,3,4-tetrahydronaphthyl)	O	CONH	N
29	phenyl	pentyl	(*S*)-1-(1,2,3,4-tetrahydronaphthyl)	O	CONH	N
30	phenyl	pentyl	piperidin-1-yl	O	CONH	N
31	phenyl	pentyl	3-(trifluoromethyl)phenyl	O	CONH	N
32	4-chlorophenyl	pentyl	1-adamantyl	O	CONH	N
33	4-chlorophenyl	pentyl	cyclohexyl	O	CONH	N
34	4-chlorophenyl	pentyl	3-(trifluoromethyl)phenyl	O	CONH	N
35	3-chlorophenyl	pentyl	1-adamantyl	O	CONH	N
36	2-chlorophenyl	pentyl	1-adamantyl	O	CONH	N
37	4-methylphenyl	pentyl	1-adamantyl	O	CONH	N
38	4-methoxyphenyl	pentyl	1-adamantyl	O	CONH	N
39	phenyl	pentyl	1-adamantyl	S	CONH	N
40	phenyl	pentyl	cyclohexyl	S	CONH	N

moiety at position 3, but differed by their substituents at position 6 of the heterocycle (i.e., methyl, *tert*-butyl, phenyl, and 4-chlorophenyl). All of these 6-substituted analogues were selective, displaying high affinity at the CB_2 receptor and low or no affinity at CB_1 receptor. Compound **11**, with a methyl at position 6, exhibits a K_i value at CB_2 receptor (20 nM) of the same magnitude as the starting compound **8** and was found to be highly selective (K_i at $CB_1 > 3000$). A similar result was

Scheme 3[a]

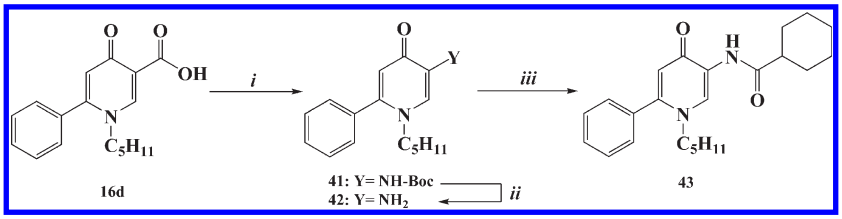

[a] Reagents and conditions: (i) DPPA, *t*-BuOK, *t*-BuOH, reflux, 12 h, 38%; (ii) (a) 5N HCl, isopropyl alcohol, rt, 14 h, (b) 10% NaOH, 95%; (iii) (a) cyclohexyl carboxylic acid, HOBt, HBTU, DIPEA, DMF, rt, 3 h, (b) **38**, rt, 12 h, 38%.

Table 2. Affinities (K_i values) of Compounds **11**, **17**−**41**, **43**, and Reference Compounds (**5**, WIN-55,212-2, CP-55,940, and **1**) towards hCB$_1$ and hCB$_2$ Cannabinoid Receptors[a]

	binding affinity K_i (nM)		
compd	hCB$_1$	hCB$_2$	selectivity ratio CB$_2$ versus CB$_1$
11	> 3000	20 ± 3	> 150
17	> 3000	29 ± 3	> 103
18	> 3000	29 ± 3	> 103
19	> 3000	414 ± 61	> 7
20	368 ± 84	14.3 ± 2.1	26
21	> 3000	> 3000	
22	626 ± 92	23.3 ± 1.9	27
23	454 ± 55	6.6 ± 0.7	69
24	> 1000	18.4 ± 1.3	> 54
25	592 ± 97	4.0 ± 0.4	148
26	596 ± 75	13.5 ± 0.9	44
27	929 ± 131	10.6 ± 1.1	88
28	131 ± 20	10.1 ± 1.1	13
29	> 1000	369 ± 41	> 3
30	> 3000	92 ± 7	> 33
31	> 3000	25.8 ± 3	> 116
32	> 1000	79 ± 7	> 13
33	> 1000	78 ± 9	> 13
34	> 1000	> 1000	
35	51.2 ± 6	1.8 ± 0.2	29
36	34.4 ± 6	0.7 ± 0.1	48
37	134 ± 19	13.2 ± 1.6	10
38	384 ± 56	91.1 ± 14	4
39	> 1000	18.8 ± 2.3	> 53
40	> 1000	48 ± 4	> 21
41	> 3000	209 ± 33	> 14
43	> 3000	51 ± 4	> 59
5	ND	51.7 ± 4.8	
WIN-55,212-2	ND	9.1 ± 0.8	
CP-55,940	ND	15.4 ± 1.4	
1	ND	20.3 ± 2.6	

[a] The K_i values were obtained from nonlinear analysis of competition curves using using [^{3}H]-SR141716A and [^{3}H]-CP-55,940 as radioligands for hCB$_1$ and hCB$_2$ cannabinoid receptors, respectively, and are expressed as mean ± SEM of at least four experiments performed in duplicate.

Table 3. Potency (EC_{50}) and Maximal Stimulation (E_{max}) of Selected Compounds and Reference Ligands on hCB$_2$ Cannabinoid Receptor[a]

	[^{35}S]-GTPγS (hCB$_2$)	
compd	EC_{50} (nM)	E_{max} (%)[b]
11	5.5 ± 1.1	148 ± 2[c]
17	12.2 ± 2.5	212 ± 3[d]
18	7.8 ± 3.5	135 ± 3[c]
20	6.5 ± 1.5	46 ± 3[e]
22	10.9 ± 2.8	37 ± 1[e]
23	5.8 ± 1.1	41 ± 2[e]
24	7.4 ± 0.9	40 ± 2[e]
25	3.2 ± 1.6	39 ± 2[e]
26	8.7 ± 0.9	33 ± [e]
27	1.9 ± 0.5	62 ± 2[e]
28	1.9 ± 0.4	42 ± 2[e]
29	60 ± 16	48 ± 3[e]
30	26 ± 6	48 ± 2[e]
31	14 ± 4	42 ± 4[e]
32	23 ± 6	42 ± 2[e]
33	22 ± 4	39 ± 2[e]
34	158 ± 42	42 ± 3[e]
39	17 ± 2	30 ± 1[e]
40	27 ± 3	45 ± 1[e]
41	164 ± 28	26 ± 3[e]
43	25 ± 3	43 ± 2[e]
5	1.8 ± 0.9	21.6 ± 2.7[e]
WIN-55,212-2	24.6 ± 1.6	207.1 ± 10.1[d]
CP-55,940	6.1 ± 2.1	230.5 ± 13.7[d]
1	145.6 ± 3	201.4 ± 7.5[d]

[a] The results are expressed as mean ± SEM of at least four experiments performed in duplicate. [b] Basal constitutive activity of the receptor has been set at a value of 100%. [c] E_{max} values between 100% and 200%indicated that the compound behaves as a partial agonist. [d] E_{max} values around 200% indicated that the compound behaves as a full agonist. [e] E_{max} values under 100% indicated that the compound behaves as an inverse agonist.

obtained for compound **17** bearing a *tert*-butyl group. Replacing the methyl or *tert*-butyl groups by a phenyl resulted in a 5-fold enhancement of the affinity (e.g., **25** with a K_i value of 4 nM), while selectivity was not altered. Introducing a chlorine atom in the para position of the phenyl ring resulted in a decrease in both selectivity and CB$_2$ affinity (compare compounds **25** and **32**). When considering their functionality, we noticed that compound **11** dose-dependently increased the [^{35}S]-GTPγS binding up to 148% with an EC_{50} value of 5.5 nM, which means that this compound behaves as a partial agonist, whereas compound **17** behaves as a potent full agonist increasing [^{35}S]-GTPγS binding to the same extent as CP-55,940 (EC_{50} = 12.2 nM and E_{max} = 212%). More surprisingly, introducing a phenyl or a 4-chlorophenyl group in place of methyl or *tert*-butyl shifted the functionality from agonist to inverse agonist because both compounds **25** and **32** decreased [^{35}S]-GTPγS binding with E_{max} values of 39% and 42%, respectively. Because the functionality switch observed within this series of compounds is an interesting feature, we decided to investigate whether the change in functionality we observed when replacing the C-6 *tert*-butyl substituent with a phenyl or 4-chlorophenyl substituent was dependent on the phenyl substituent. Therefore we synthesized four additional compounds characterized by differently substituted phenyls (**35**−**38**) and evaluated their affinity and functionality. These compounds show a similar affinity for the CB$_2$ receptor when compared to **25**, although they are marginally less selective (Table 2). When looking at their functionality, they too behave as inverse agonists decreasing [^{35}S]-GTPγS binding (E_{max} values of 75 ± 2%, 88 ± 1%, and 75 ± 5% for **35**, **36**,

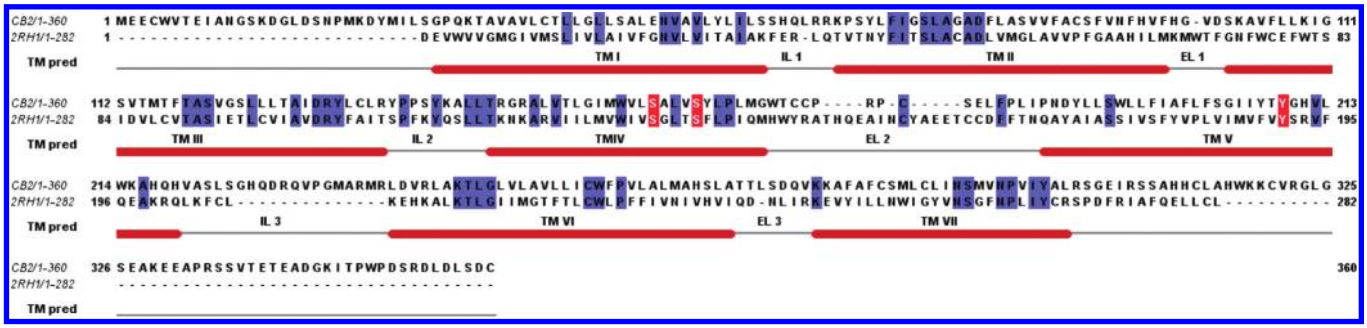

Figure 1. Sequence alignment between the model human CB_2 receptor and the crystal template sequences. This JalView[64] graphical representation shows the alignment between the whole CB_2 model sequence and the partial sequence (without N-terminal, C-terminal, and IL3 regions) of the X-ray β2-adrenergic receptor (PDB 2RH1). The identical conserved amino acids and relevant CB_2 features Ser4.53, Ser4.57, and Tyr5.58 are respectively displayed as blue and red overlined residues. The TM domains deduced from crytstal template are annotated in the "TM pred" section.

and **37**, respectively), although the 4-methoxyphenyl substituted 4-oxo-1,4-dihydropyridine behaves as a partial agonist (E_{max} = 148 ± 4%). Taken together, these observations suggest that the C-6 substituent of the 4-oxo-1,4-dihydropyridine ring appears to be crucial for the control of functionality at CB_2 receptor and also modulates affinity, efficacy, and selectivity.

Because derivative **25** combines a good affinity with the highest selectivity, we decided to retain the C-6 phenyl moiety and to develop a series of CB_2 inverse agonists with various *N*-1 and 3-carboxamido substituents. Therefore, the replacement of the *n*-pentyl chain by *n*-ethyl, *n*-butyl, or *n*-hexyl groups resulted in moderate to strong reduction of the affinity (see compounds **19**, **24**, **26**) while introducing a phenyl (compound **21**) completely abolished the CB_2 affinity. Taken together, these data, in accordance with our previous work,[40] clearly emphasize that the affinity toward the CB_2 receptor is very sensitive to *N*-1 substituent, with *n*-pentyl chain being the preferred one.

Next, we investigated the modification of the amide substituent because it seems to affect affinity toward both cannabinoid receptors. It was shown for the 4-oxo-1,4-dihydroquinoline-3-carboxamide derivatives that bulky aliphatic substituents (especially adamantyl) are favorable for CB_2 affinity and selectivity,[40,41] and compounds **11**, **17**, and **25** confirmed this observation. Enhancement of adamantyl lipophilicity by introducing two methyl groups in position 3 and 5 of the adamantyl ring (compound **23**) improved neither affinity nor efficacy at CB_2 receptor but enhanced CB_1 receptor affinity. When the adamantyl moiety was positioned further away from the 4-oxo-1,4-dihydropyridine core (by a methylene link) leading to compound **22**, affinity at CB_2 decreased by 6-fold. However, when a methyl group was added on the methylene link, the affinity for both cannabinoid receptors was increased (compare **22** and **20**). When a phenyl group was placed at position 6 of the 4-oxo-1,4-dihydropyridine ring, the replacement of the adamantyl moiety by a less bulky aliphatic group like cyclohexyl induced a slight decrease in affinity (compare **25** and **27**). However, no effect was observed when a *tert*-butyl or a 4-chlorophenyl was placed at position 6 (compare for instance **17** and **18** or **32** and **33**).

Next, we prepared compound **30**, with a piperidyl group on the amide moiety, which showed a K_i value of 92 nM at CB_2 receptor and was found inactive at CB_1. Introducing an aromatic moiety, especially the 3-(trifluoromethyl)phenyl group, in place of adamantyl caused a reduction in affinity and efficacy at CB_2. This is illustrated for instance by compounds **25** and **31**, which exhibit K_i values of 4 and 26 nM, respectively.

By analogy with 4-oxo-1,4-dihydroquinoline-3-carboxamide derivatives, we introduced a chiral center on the carboxamido function in order to assess the effect of stereoselectivity on the affinity, selectivity, and functionality of our inverse agonist series. Therefore, we prepared two compounds characterized by the 1-(1,2,3,4-tetrahydronaphthyl) moiety, **28** represents the (*R*) enantiomer and **29** the (*S*) enantiomer. The eutomer (compound **28**) of this novel series exhibited more than 30-fold higher affinity for the CB_2 receptor than the distomer (compound **29**). In accordance with our earlier work, a stereoselectivity is observed with the (*R*) enantiomer exhibiting a better affinity and efficacy than the (*S*) enantiomer. Furthermore, compound **28** as well as compound **27** are the most potent compounds of our series, with EC_{50} values of 1.9 nM.

As expected, the 3-carboxamido substituent is an important parameter for the affinity, efficacy, and selectivity. However, and opposite to what we found for the C-6 position, this modification did not affect the functionality because, regardless the carboxamido substituent, all the compounds retained their respective functionality.

When looking at the amide link of **27**, we found that the reverse amide **43** has 5-fold lower affinity as compared to the amide analogue. In a similar manner, the carbamate intermediate **41**, which can be regarded as an analogue of compound **43** wherein its cyclohexyl moiety is replaced by a *tert*-butoxy group, displayed a lower affinity with a K_i value of 209 nM at CB_2 and no affinity at CB_1.

We also introduced a thioketone in place of the carbonyl of 4-oxo-1,4-dihydropyridine core, leading to compounds **39** and **40**. Albeit this frequent substitution has already been proved to affect the affinity or functionality of some cannabinoid ligands,[47,41] we found here that this modification resulted in a 5-fold reduction of the affinity and had no effect on the functionality.

In Silico Insights from an Inactive State Model of the CB_2 Receptor

The inactive state of the human CB_2 apo-receptor was built from the homologous crystal template of the human β2-adrenergic receptor (Figure 1), as specified in the Experimental Section. Thus, the modeled CB_2 receptor should be in its inactive state because the human β2-adrenergic receptor template used was cocrystallized with a high-affinity inverse agonist.[48−51]

As illustrated in Figure 2, the resulting ligand binding site is restricted by transmembrane domain (TM) III, IV, V, VI, and VII, as well as extracellular loops (EL) 2 and 3. The resulting docking poses of both compounds **17** and **25** revealed a consensual binding mode, as the five best ones were superimposed within a 1.5 Å root-mean-square deviation (rmsd) (Figure 3). Both compounds **17** and **25** are anchored by hydrogen bonds with Tyr5.39 (Tyr190) and Phe183 backbone of EL2. The pentyl chains spread out in a lipophilic pocket defined by Phe91, Phe94, Phe106, Ile110, Val113, and Leu182. The adamantyl groups fit in the extracellular region particularly EL2, whereas the C-6 *tert*-butyl or phenyl substituents of compounds **17** and **25**, respectively, orient toward the bottom of the pocket defined by an aromatic cage including Phe3.36 (Phe117), Trp5.43 (Trp194), and Trp6.48 (Trp258). Trp6.48 is included in the CWXP pattern of helix 6 and is strictly conserved among the class A GPCRs. Trp6.48 and adjacent side chains have been shown to undergo conformational transitions as a "rotamer toggle switch" during the activation of rhodopsin[52−54] and β2-adrenergic receptors.[55] This "rotamer toggle switch" has also been shown to be critical for the activation of the CB_1 receptor with specific contacts between Phe3.36 and Trp6.48 in the inactive state, which are broken during the activation, leading to a χ_1 rotamer switch (F3.36 trans(180°)/W6.48 g+(−60°)) → (F3.36 g+, W6.48 trans).[56] As observed in the CB_2 receptor bound to the compound **25** (Figure 3A), Phe3.36 and Trp6.48 form a $\pi-\pi$ face-to-face interaction, whereas the C-6 phenyl substituent of compound **25** establishes edge-to-face aromatic interactions with Trp6.48. During the MD simulation, the placement of both ligands was examined by monitoring the distance between the C-6 substituents of the ligands and the side chain of Trp6.48 (Figure 4). Taking into account the distance between the closest carbon atoms in the minimized complex at $t = 0$, the simulation shows that the distance implying the C-6 phenyl group of compound **25** tends to converge toward a distance of 4 Å, whereas the distance between the C-6 *tert*-butyl substituent of compound **17** and the side chain of Trp6.48 does not converge and varies between 5 and 8 Å. The preservation of the aromatic cluster between the C-6 substituent of compound **25** and Trp6.48 is also depicted by monitoring the receptor−ligand binding energy during the MD simulation (Figure 4). Indeed, the binding energy of the complex with compound **25** ranges from −65 to −55 kcal/mol and is thus more stabilizing

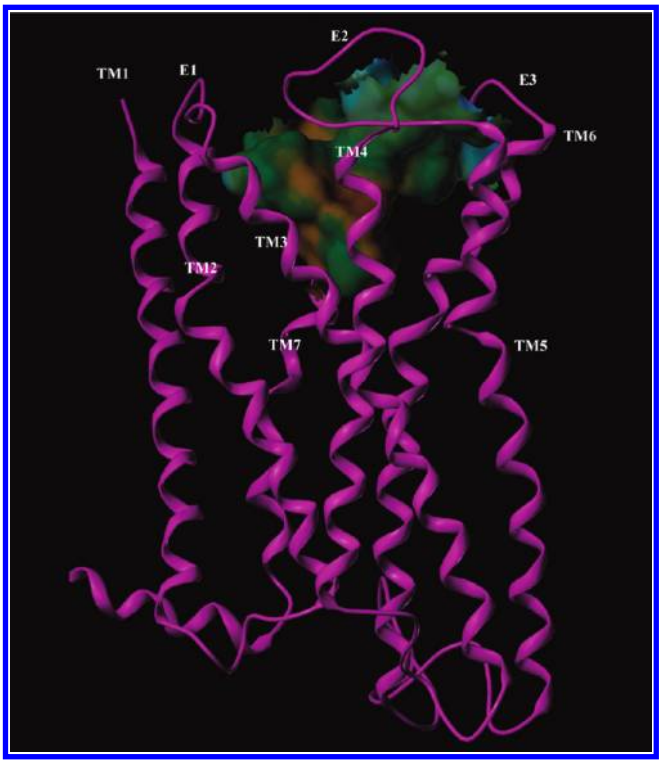

Figure 2. Homology model of the CB_2 apo-receptor. A global overview of the complex model is represented where the binding site is displayed as a solvent-accessible surface colored from blue for polar regions to brown for hydrophobic regions.

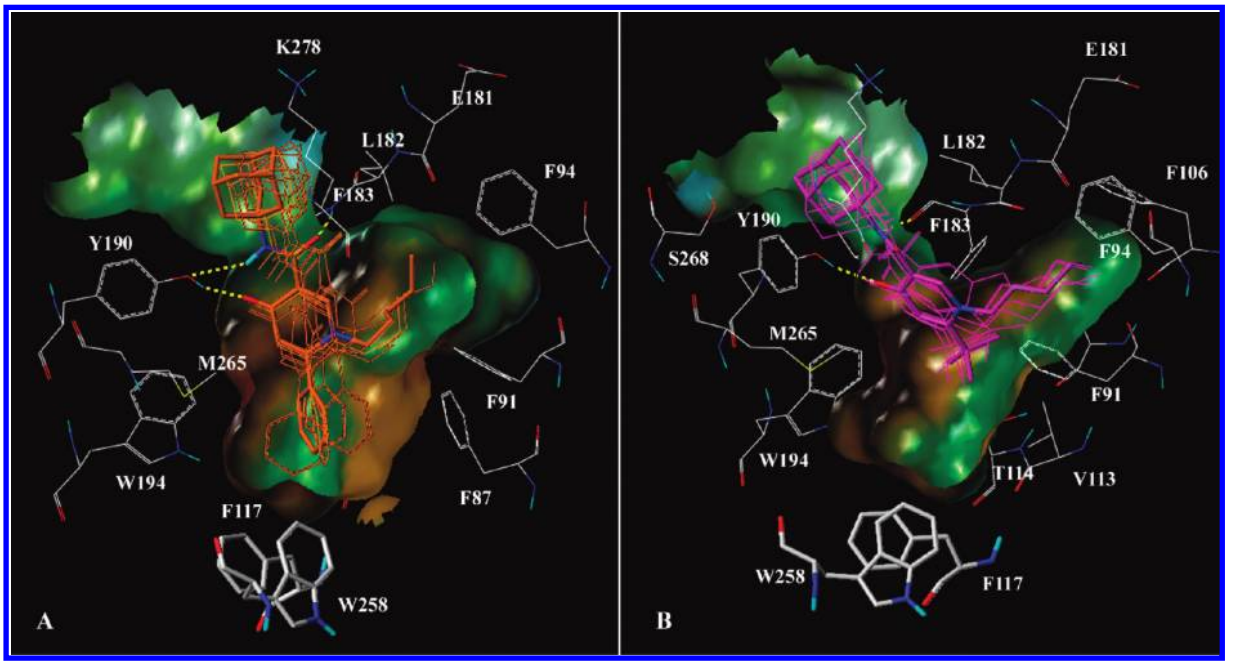

Figure 3. Ligand-bound states of the CB_2 receptor with compounds **25** (A) and **17** (B). The best docking poses for each ligand are displayed as lines, whereas the ligand pose carried out from energy minimization is illustrated as sticks. The hydrogen bonds figure as yellow dashed lines.

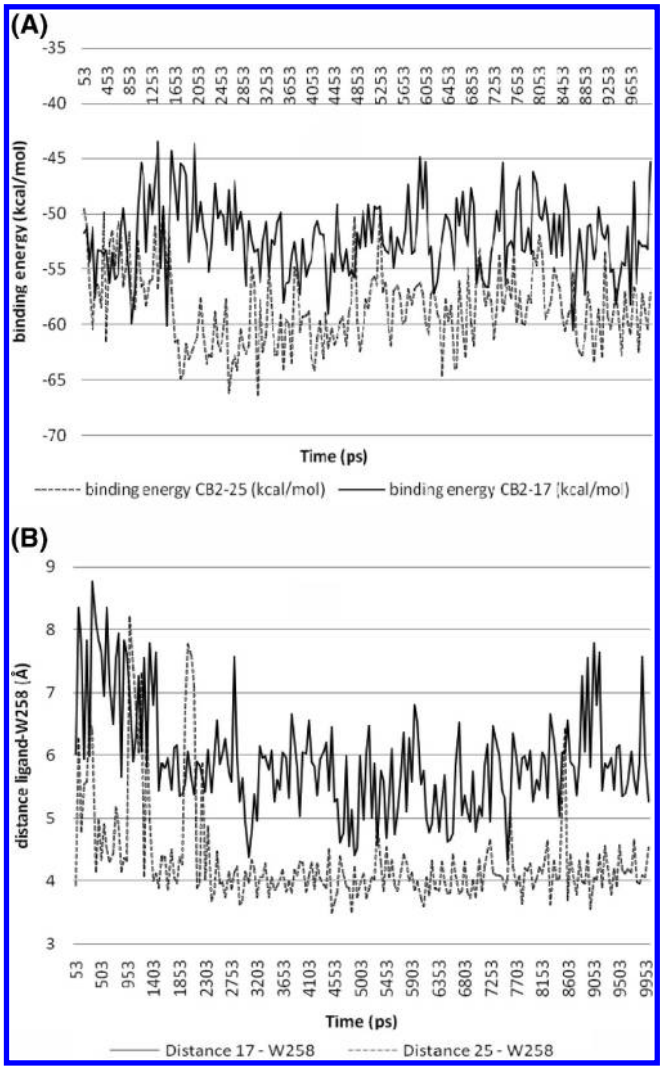

Figure 4. Analysis of molecular dynamics simulations. Binding energy between **17** and **25** with the CB_2 receptor was plotted (A) as well as the distance between the less buried carbon atom of Trp258 (W258) side chain and the more buried carbon atom of the ligand (B).

than the complex, including compound **17**, for which the binding energy ranges from −55 to −45 kcal/mol.

Even though the duration of the simulation is not long enough to observe a conformational switch of Trp6.48 χ_1 torsion from the g(+) (−60°) toward its trans conformation (180°), these results suggest that the phenyl substituent at the C-6 position of compound **25** confers the inverse agonist profile by stabilizing the χ_1 torsion of Trp6.48 side chain in its inactive g(+) conformation and thus could prevent its transition toward the trans conformation thought to be essential for the receptor activation.

Conclusion

We have synthesized a series of selective CB_2 receptor ligands based on a 4-oxo-1,4-dihydropyridine scaffold. Binding assays showed that the nature of substituents around the heterocycle strongly impacts on both affinity and functionality. We have identified the C-6 substituent as crucial in controlling the functionality of this series of compounds because replacing an alkyl group by a phenyl group switched the functionality from agonist to inverse agonist. Conversely, we demonstrate that substituents at *N*-1 and C-3 position are crucial for affinity but not for functionality. Using a β2-adrenergic receptor-based CB_2 receptor model, we suggest that the phenyl at C-6 confers the inverse agonist profile by blocking the χ_1 torsion of Trp6.48 side chain in its inactive conformation. Overall, the data presented here show that the 4-oxo-1,4-dihydropyridine ring is a highly effective scaffold for the design of new CB_2 receptor ligands. Moreover, the novel selective CB_2 ligands reported here will be useful tools for characterizing the functions of CB_2 receptor.

Experimental Section

Chemistry. All commercial reagents and solvents were used without further purification. Analytical thin-layer chromatography was performed on precoated Kieselgel 60F_{254} plates (Merck); the spots were located by UV (254 and 366 nm) and/or with iodine. Silica gel 60 230−400 mesh purchased from Merck was used for column chromatography. Alumina silica gel (neutral) 150 mesh purchased from Sigma Aldrich was used for column chromatography for purification of compound **13c**. Preparative thick-layer chromatography (TLC) was performed using silica gel from Merck, the compounds were extracted from the silica using $CHCl_3$/MeOH (8:2, v/v). All melting points were determined with a Büchi 535 capillary apparatus and remain uncorrected. ^{1}H NMR spectra were obtained using a Brüker 300 MHz spectrometer, chemical shifts (δ) are expressed in ppm relative to tetramethylsilane used as an internal standard, *J* values are in hertz, and the splitting patterns are designated as follows: s, singlet; d, doublet; t, triplet; m, multiplet. All compounds were analyzed by HPLC-MS on a HPLC combined with a Surveyor MSQ (Thermo Electron) equipped with an APCI-source. All tested compounds showed a purity of >96% in $APCI^+$ mode.

3-(Dimethylaminomethylene)-6-methyl-4-oxo-2-pyrone **9** was prepared according to a procedure already described.[42,43] Compound **9** crystallizes in a mixture of toluene/cyclohexane (2:8, v/v).

The ethyl 2-[(dimethylamino)methylene]-3-oxobutanoate **12**, pyran-4-ones **13a** (ethyl 6-*tert*-butyl-4-oxo-4*H*-pyran-3-carboxylate) and **13b** (ethyl 4-oxo-6-phenyl-4*H*-pyran-3-carboxylate) and pyridin-4-one **14f** (ethyl 4-oxo-1,6-diphenyl-1,4-dihydropyridine-3-carboxylate) were obtained using the procedures previously described[44] with minor modifications. In our case, pyran-4-ones **13a−g** were unstable on silica gel and could not be purified even by flash chromatography. We found that pyran-4-ones **13a−b and 13d−g** crystallize in diethyl ether at low temperature under reduced pressure.

6-Methyl-4-oxo-1-pentyl-1,4-dihydropyridine-3-carboxylic Acid (10). To a stirred solution of compound **9** (0.2 g; 1.1 mmol) in anhydrous ethanol (EtOH) (10 mL) were added under nitrogen atmosphere, potassium *tert*-butoxide (0.17 g; 1.7 mmol), and *n*-pentylamine (0.25 mL; 2.2 mmol). This mixture was refluxed under nitrogen for 12 h. EtOH was removed under reduced pressure and the residue dissolved in water. The aqueous phase was washed with ethyl acetate (EtOAc), and the resulting solution was carefully acidified with a 1 N HCl solution to pH 2 and extracted with EtOAc. The combined organic extracts were washed with H_2O, dried over $MgSO_4$, and the solvent removed under reduced pressure to afford pure **10** as a white solid (0.18 g, 73%); mp 126 °C. ^{1}H NMR ($CDCl_3$) δ 16.61 (s, 1H), 8.43 (s, 1H), 6.58 (s, 1H), 3.97 (t, 2H, J = 7.9 Hz), 2.45 (s, 3H), 1.80 (m, 2H), 1.38 (m, 4H), 0.93 (t, 3H, J = 6.8 Hz). LC-MS ($APCI^+$) m/z 224.2 (MH^+).

General Procedure for the Preparation of Ethyl 6-Aryl-4-oxo-4*H*-pyran-3-carboxylate (13c−13g). These compounds were obtained using the same methodology as already described.[44]

Ethyl 6-(4-Chlorophenyl)-4-oxo-4*H*-pyran-3-carboxylate (13c). Compound **13c** was purified by neutral silica−alumina gel chromatography (dichloromethane/ethyl acetate 1:1, v/v); beige

solid (52%); mp 155 °C. ^{1}H NMR ($CDCl_3$) δ 8.58 (s, 1H), 7.7 (d, 2H, J = 9.1 Hz), 7.5 (d, 2H, J = 9.1 Hz), 6.84 (s, 1H), 4.40 (q, 2H, J = 7.0 Hz), 1.41 (t, 3H, J = 7.0 Hz). LC-MS (APCI$^+$) m/z 279.4 (MH^+).

Ethyl 6-(3-Chlorophenyl)-4-oxo-4*H*-pyran-3-carboxylate (13d). Beige solid (57%); mp 118 °C. ^{1}H NMR ($CDCl_3$) δ 8.59 (s, 1H), 7.76 (s, 1H), 7.65 (d, 2H, J = 7.6 Hz), 7.48 (m, 2H), 6.86 (s, 1H), 4.40 (q, 2H, J = 7.0 Hz), 1.41 (t, 3H, J = 7.0 Hz). LC-MS (APCI$^+$) m/z 279.0 (MH^+).

Ethyl 6-(2-Chlorophenyl)-4-oxo-4*H*-pyran-3-carboxylate (13e). Beige solid (35%). ^{1}H NMR ($CDCl_3$) δ 8.39 (s, 1H), 7.21 (m, 4H), 6.49 (s, 1H), 4.12 (q, 2H, J = 7.0 Hz), 1.12 (t, 3H, J = 7.0 Hz). LC-MS (APCI$^+$) m/z 279.1 (MH^+).

Ethyl 6-(4-Methylphenyl)-4-oxo-4*H*-pyran-3-carboxylate (13f). Beige solid (63%); mp 96 °C. ^{1}H NMR ($CDCl_3$) δ 8.57 (s, 1H), 7.67 (d, 2H, J = 8.2 Hz), 7.32 (d, 2H, J = 8.2 Hz), 6.83 (s, 1H), 4.40 (q, 2H, J = 7.1 Hz), 1.41 (t, 3H, J = 7.1 Hz). LC-MS (APCI$^+$) m/z 259.1 (MH^+).

Ethyl 6-(4-Methoxyphenyl)-4-oxo-4*H*-pyran-3-carboxylate (13g). Yellow solid (57%); mp 134 °C. ^{1}H NMR ($CDCl_3$) δ 8.56 (s, 1H), 7.70 (d, 2H, J = 9.0 Hz), 7.0 (d, 2H, J = 9.0 Hz), 6.77 (s, 1H), 4.40 (q, 2H, J = 7.0 Hz), 3.88 (s, 3H) 1.39 (t, 3H, J = 7.0 Hz). LC-MS (APCI$^+$) m/z 275.1 (MH^+).

Ethyl 6-*tert*-Butyl-4-oxo-1-pentyl-1,4-dihydropyridine-3-carboxylate (14a). A solution of pyrone ester (**13a**) (3 g, 13.4 mmol), *n*-pentylamine (3.1 mL, 26.7 mmol) in EtOH (60 mL) and acetic acid (AcOH) (40 mL) was refluxed for 4 h. The mixture was cooled to room temperature and the solvents were distilled off to leave a brown oil. Water was added and the product was extracted with CH_2Cl_2. The crude oil was chromatographed on silica gel (dichloromethane/methanol 98:2) to give a rust colored oil (2.24 g, 57%); ^{1}H NMR ($CDCl_3$) δ 8.12 (s, 1H), 6.55 (s, 1H), 4.38 (q, 2H, J = 7.1 Hz), 4.02 (t, 2H, J = 8.3 Hz), 1.81 (m, 2H), 1.40−1.34 (m, 16H), 0.94 (t, 3H, J = 6.7 Hz). LC-MS (APCI$^+$) m/z 294.4 (MH^+).

General Procedure for the Preparation of Ethyl 1-Alkyl-6-aryl-4-oxo-1,4-dihydropyridine-3-carboxylate (14b−e, 14g−k). To a solution of pyrone in EtOH/AcOH (3:1, v/v) was added, slowly, the appropriate alkylamine or aniline (2 equiv) at 5 °C. The mixture was refluxed for 1 h. After cooling to room temperature, solvents were evaporated and the residue partitioned in H_2O−$CHCl_3$. The organic phase was washed both with water and brine, dried, and evaporated to leave an oil. The latter was chromatographed on silica gel to afford pure product.

Ethyl 1-Ethyl-4-oxo-6-phenyl-1,4-dihydropyridine-3-carboxylate (14b). Purification by silica gel chromatography (dichloromethane/ethyl acetate 1:1); beige solid (77%); mp 159 °C. ^{1}H NMR ($CDCl_3$) δ 8.41 (s, 1H), 7.50 (m, 5H), 6.07 (s, 1H), 4.22 (q, 2H, J = 6.9 Hz), 3.81 (q, 2H, J = 7.4 Hz), 1.26 (t, 3H, J = 6.9 Hz), 1.04 (t, 3H, J = 7.4 Hz). LC-MS (APCI$^+$) m/z 272.1 (MH^+).

Ethyl 1-Butyl-4-oxo-6-phenyl-1,4-dihydropyridine-3-carboxylate (14c). Purification by silica gel chromatography (dichloromethane/ethyl acetate 1:1, v/v); brown oil (74%). ^{1}H NMR ($CDCl_3$) δ 8.22 (s, 1H), 7.48 (m, 3H) 7.32 (m, 2H), 6.42 (s, 1H), 4.39 (q, 2H, J = 7.2 Hz), 3.74 (t, 2H, J = 7.6 Hz), 1.52 (m, 2H), 1.38 (t, 3H, J = 7.2 Hz), 1.12 (m, 2H), 0.75 (t, 3H, J = 7.4 Hz). LC-MS (APCI$^+$) m/z 300.2 (MH^+).

Ethyl 4-Oxo-1-pentyl-6-phenyl-1,4-dihydropyridine-3-carboxylate (14d). Purification by silica gel chromatography (dichloromethane/ethyl acetate 1:1, v/v); brown oil (71%). ^{1}H NMR (DMSO-d_6) δ 8.40 (s, 1H), 7.51 (m, 5H), 6.08 (s, 1H), 4.22 (q, 2H, J = 7.0 Hz), 3.81 (t, 2H, J = 7.6 Hz), 1.38 (m, 2H), 1.26 (t, 3H, J = 7.0 Hz), 1.02 (m, 4H), 0.69 (t, 3H, J = 7.0 Hz). LC-MS (APCI$^+$) m/z 314.2 (MH^+).

Ethyl 4-Oxo-1-hexyl-6-phenyl-1,4-dihydropyridine-3-carboxylate (14e). Purification by silica gel chromatography (dichloromethane/ethyl acetate 1:1, v/v); brown oil (68%). ^{1}H NMR ($CDCl_3$) δ 8.22 (s, 1H), 7.41 (m, 5H), 6.08 (s, 1H), 4.19 (q, 2H, J = 6.9 Hz), 3.93 (t, 2H, J = 7.3 Hz), 1.26−1.02 (m, 11H), 0.73 (t, 3H, J = 7.1 Hz). LC-MS (APCI$^+$) m/z 328.2 (MH^+).

Ethyl 6-(4-Chlorophenyl)-4-oxo-1-pentyl-1,4-dihydropyridine-3-carboxylate (14g). Purification by silica gel chromatography (dichloromethane/methanol 9:1, v/v); yellow oil (75%). ^{1}H NMR ($CDCl_3$) δ 8.22 (s, 1H), 7.50 (d, 2H, J = 8.8 Hz), 7.30 (d, 2H, J = 8.8 Hz), 6.40 (s, 1H), 4.40 (q, 2H, J = 7.1 Hz), 3.72 (t, 2H, J = 7.7 Hz), 1.55 (m, 2H), 1.40 (t, 3H, J = 7.1 Hz), 1.18 (m, 4H), 0.82 (t, 3H, J = 7.0 Hz). LC-MS (APCI$^+$) m/z 348.2 (MH^+).

Ethyl 6-(3-Chlorophenyl)-4-oxo-1-pentyl-1,4-dihydropyridine-3-carboxylate (14h). Purification by silica gel chromatography (dichloromethane/methanol 9:1, v/v); yellow oil (63%). ^{1}H NMR ($CDCl_3$) δ 8.22 (s, 1H), 7.48 (m, 2H), 7.34 (s, 1H), 7.24 (d, 2H, J = 7.6 Hz), 6.41 (s, 1H), 4.40 (q, 2H, J = 7.1 Hz), 3.72 (t, 2H, J = 7.7 Hz), 1.55 (m, 2H), 1.40 (t, 3H, J = 7.1 Hz), 1.13 (m, 4H), 0.82 (t, 3H, J = 7.0 Hz). LC-MS (APCI$^+$) m/z 348.1 (MH^+).

Ethyl 6-(2-Chlorophenyl)-4-oxo-1-pentyl-1,4-dihydropyridine-3-carboxylate (14i). Purification by silica gel chromatography (dichloromethane/methanol 9:1, v/v); yellow oil (45%). ^{1}H NMR ($CDCl_3$) δ 8.10 (s, 1H), 7.17 (m, 4H), 6.12 (s, 1H), 4.10 (q, 2H, J = 7.1 Hz), 3.78 (t, 2H, J = 7.7 Hz), 1.32 (m, 2H), 1.12 (t, 3H, J = 7.1 Hz), 0.86 (m, 4H), 0.51 (t, 3H, J = 7.0 Hz). LC-MS (APCI$^+$) m/z 348.1 (MH^+).

Ethyl 6-(4-Methylphenyl)-4-oxo-1-pentyl-1,4-dihydropyridine-3-carboxylate (14j). Purification by silica gel chromatography (dichloromethane/methanol 9:1, v/v); yellow oil (75%). ^{1}H NMR ($CDCl_3$) δ 8.02 (s, 1H), 6.98 (q, 2H, J = 6.9 Hz), 6.10 (s, 1H), 4.06 (q, 2H, J = 7.1 Hz), 3.57 (t, 2H, J = 7.4 Hz), 2.11 (s, 3H), 1.27 (m, 2H), 1.07 (t, 3H, J = 7.1 Hz), 0.82 (m, 4H), 0.48 (t, 3H, J = 6.9 Hz). LC-MS (APCI$^+$) m/z 328.2 (MH^+).

Ethyl 6-(4-Methoxyphenyl)-4-oxo-1-pentyl-1,4-dihydropyridine-3-carboxylate (14k). Purification by silica gel chromatography (dichloromethane/methanol 9:1, v/v); yellow oil (57%). ^{1}H NMR ($CDCl_3$) δ 8.15 (s, 1H), 7.20 (d, 2H, J = 8.8 Hz), 6.90 (d, 2H, J = 8.8 Hz), 6.31 (s, 1H), 4.29 (q, 2H, J = 7.1 Hz), 3.72 (t, 2H, J = 7.6 Hz), 3.79 (s, 3H), 1.52 (m, 2H), 1.34 (t, 3H, J = 7.1 Hz), 1.06 (m, 4H), 0.72 (t, 3H, J = 7.0 Hz). LC-MS (APCI$^+$) m/z 344.2 (MH^+).

Ethyl 1-Pentyl-6-phenyl-4-thioxo-1,4-dihydropyridine-3-carboxylate (15). A mixture of **14d** (2.6 g, 8.3 mmol) and phosphorus pentasulfide (3.7 g, 16.6 mmol) was refluxed for 12 h in pyridine (80 mL). After cooling to room temperature, the solvent was removed under reduced pressure and the residue was partitioned in H_2O−EtOAc. The organic layer was washed with brine, dried, and concentrated under reduced pressure to leave a rust-colored oil. The latter was purified by silica gel chromatography (cyclohexane/ethyl acetate 9:1, v/v) to give an orange oil (2.46 g, 90%). ^{1}H NMR (DMSO-d_6) δ 8.22 (s, 1H), 7.54 (m, 5H), 7.06 (s, 1H), 4.26 (q, 2H, J = 7.0 Hz), 3.85 (t, 2H, J = 7.6 Hz), 1.45 (m, 2H), 1.28 (t, 3H, J = 7.0 Hz), 1.03−0.98 (m, 4H), 0.70 (t, 3H, J = 6.7 Hz). LC-MS (APCI$^+$) m/z 330.8 (MH^+).

General Procedure for the Preparation of Carboxylic Acids (16a−h). Esters **14a−g** and **15** were dissolved in ethanol and 2.5 N NaOH (v/v). The mixture was refluxed for 6 h. After cooling to room temperature, EtOH was removed under reduced pressure and the residue was dissolved in water and washed with EtOAc. The aqueous phase was acidified (1 N HCl, pH 2) and extracted with EtOAc. The combined organic extracts were washed with water and brine, dried over $MgSO_4$, and concentrated under reduced pressure to afford essentially pure carboxylic acids **16a−h**.

6-*tert*-Butyl-4-oxo-1-pentyl-1,4-dihydropyridine-3-carboxylic Acid (16a). Beige powder (77%); mp 89 °C. ^{1}H NMR (DMSO-d_6) δ 11.97 (s, 1H), 8.66 (s, 1H), 6.68 (s, 1H), 4.31 (t, 2H, J = 8.2 Hz), 1.73 (m, 2H), 1.41 (s, 9H), 1.32 (m, 4H), 0.87 (t, 3H, J = 6.7 Hz). LC-MS (APCI$^+$) m/z 266.3 (MH^+).

1-Ethyl-4-oxo-6-phenyl-1,4-dihydropyridine-3-carboxylic Acid (16b). Beige powder (96%); mp 108 °C. ^{1}H NMR ($CDCl_3$) δ 12.56 (s, 1H), 8.51 (s, 1H), 7.54 (m, 5H), 6.09 (s, 1H), 4.02 (q, 2H, J = 7.4 Hz), 1.17 (t, 3H, J = 7.4 Hz). LC-MS (APCI$^+$) m/z 244.2 (MH^+).

1-Butyl-4-oxo-6-phenyl-1,4-dihydropyridine-3-carboxylic Acid (16c). White powder (92%); mp 121 °C. ^{1}H NMR (DMSO-d_6)

δ 16.35 (s, 1H), 8.87 (s, 1H), 7.56 (m, 5H), 6.63 (s, 1H), 4.03 (t, 2H, J = 7.6 Hz), 1.43 (m, 2H),1.03 (m, 2H), 0.63 (t, 3H, J = 7.4 Hz). LC-MS (APCI$^+$) m/z 272.1 (MH$^+$).

4-Oxo-1-pentyl-6-phenyl-1,4-dihydropyridine-3-carboxylic Acid (16d). Purification by silica gel chromatography (dichloromethane/ethyl acetate 1:1, v/v); white powder (88%); mp 115 °C. ^{1}H NMR ($CDCl_3$) δ 13.5 (s, 1H), 8.4 (s, 1H), 7.48 (m, 5H), 6.08 (s, 1H), 3.81 (t, 2H, J = 7.1 Hz), 1.38 (m, 2H), 1.02−0.97 (m, 4H), 0.69 (t, 3H, J = 7.0 Hz). LC-MS (APCI$^+$) m/z 286.1 (MH$^+$).

1-Hexyl-4-oxo-6-phenyl-1,4-dihydropyridine-3-carboxylic Acid (16e). Purification by silica gel chromatography (dichloromethane/ethyl acetate 1:1, v/v); beige oil (86%). ^{1}H NMR (DMSO-d_6) δ 16.35 (s, 1H), 8.88 (s, 1H), 7.56 (m, 5H), 6.63 (s, 1H), 4.02 (t, 2H, J = 7.6 Hz), 1.43−0.85 (m, 8H), 0.73 (t, 3H, J = 7.2 Hz). LC-MS (APCI$^+$) m/z 300.1 (MH$^+$).

4-Oxo-1,6-diphenyl-1,4-dihydropyridine-3-carboxylic Acid (16f). White powder (94%); mp 182 °C. ^{1}H NMR ($CDCl_3$) δ 13.20 (s, 1H), 8.76 (s, 1H), 7.42−7.21 (m, 10H), 6.82 (s, 1H). LC-MS (APCI$^+$) m/z 292.3 (MH$^+$).

6-(4-Chlorophenyl)-4-oxo-1-pentyl-1,4-dihydropyridine-3-carboxylic Acid (16g). White powder (86%); mp 184 °C. ^{1}H NMR ($CDCl_3$) δ 13.88 (s, 1H), 8.58 (s, 1H), 7.7 (d, 2H, J = 9.1 Hz), 7.5 (d, 2H, J = 9.1 Hz), 6.84 (s, 1H), 4.01 (t, 2H, J = 7.0 Hz), 1.52 (m, 2H), 1.26 (m, 4H), 1.02 (t, 3H, J = 6.9 Hz). LC-MS (APCI$^+$) m/z 320.5 (MH$^+$).

6-(3-Chlorophenyl)-4-oxo-1-pentyl-1,4-dihydropyridine-3-carboxylic Acid (16h). Beige powder (70%); mp 82 °C. ^{1}H NMR (MeOD-d_4) δ 8.80 (s, 1H), 7.61 (m, 3H), 7.50 (d, 2H, J = 7.3 Hz), 6.69 (s, 1H), 4.03 (t, 2H, J = 7.0 Hz), 1.63 (m, 2H), 1.15 (m, 4H), 0.81 (t, 3H, J = 6.9 Hz). LC-MS (APCI$^+$) m/z 320.0 (MH$^+$).

6-(2-Chlorophenyl)-4-oxo-1-pentyl-1,4-dihydropyridine-3-carboxylic Acid (16i). Yellow solid (66%); mp 153 °C. ^{1}H NMR (MeOD-d_4) δ 8.84 (s, 1H), 7.47 (m, 4H), 6.67 (s, 1H), 4.03 (t, 2H, J = 7.0 Hz), 1.61 (m, 2H), 1.12 (m, 4H), 0.78 (t, 3H, J = 6.9 Hz). LC-MS (APCI$^+$) m/z 320.1 (MH$^+$).

6-(4-Methylphenyl)-4-oxo-1-pentyl-1,4-dihydropyridine-3-carboxylic Acid (16j). Yellow solid (81%); mp 68 °C. ^{1}H NMR (MeOD-d_4) δ 8.77 (s, 1H), 7.39 (q, 4H, J = 6.9 Hz), 6.59 (s, 1H), 4.07 (t, 2H, J = 7.0 Hz), 2.42 (s, 3H), 1.59 (m, 2H), 1.10 (m, 4H), 0.77 (t, 3H, J = 6.9 Hz). LC-MS (APCI$^+$) m/z 300.1 (MH$^+$).

6-(4-Methoxyphenyl)-4-oxo-1-pentyl-1,4-dihydropyridine-3-carboxylic Acid (16k). White solid (85%); mp 73 °C. ^{1}H NMR (MeOD-d_4) δ 8.76 (s, 1H), 7.45 (d, 2H, J = 8.1 Hz), 7.10 (d, 2H, J = 8.1 Hz), 6.61 (s, 1H), 4.09 (t, 2H, J = 7.0 Hz), 3.87 (s, 3H), 1.60 (m, 2H), 1.13 (m, 4H), 0.77 (t, 3H, J = 6.9 Hz). LC-MS (APCI$^+$) m/z 316.1 (MH$^+$).

1-Pentyl-6-phenyl-4-thioxo-1,4-dihydropyridine-3-carboxylic Acid (16l). Purification by silica gel chromatography (dichloromethane/ethyl acetate 1:1, v/v); orange powder (84%); mp 108 °C. ^{1}H NMR (DMSO-d_6) δ 13.75 (s, 1H), 9.00 (s, 1H), 7.59 (m, 5H), 7.40 (s, 1H), 4.10 (t, 2H, J = 8.4 Hz), 1.49 (m, 2H), 1.02 (m, 4H), 0.69 (t, 3H, J = 6.7 Hz). LC-MS (APCI$^+$) m/z 302.1 (MH$^+$).

General Procedure for the Preparation of Carboxamides (11 and 17−40). To a solution of carboxylic acid **10** and **16a−l** in dry DMF were added *N*,*N*-diisopropylethylamine (DIPEA) (3 equiv) and the coupling agents 1-hydroxybenzotriazole (HOBt) (0.5 equiv), 2-(1*H*-benzotriazol-1-yl)-1,1,3,3-tetramethyluronium hexafluorophosphate (HBTU) (1.5 equiv). The resulting mixture was stirred at room temperature until thin-layer chromatography showed the starting material to be consumed (ca. 3 h). The appropriate amine (1.5 equiv) was then added, and the solution was stirred at room temperature for 12 h. The solvent was removed under reduced pressure and the residue taken up in water and extracted with CH_2Cl_2. The organic phase was washed with saturated aqueous $NaHCO_3$ solution, with 1 N aqueous HCl, and water. The organic extract was dried over $MgSO_4$ and concentrated in vacuo to a brown oil. The crude material was purified by TLC using the appropriate eluent (dichloromethane/methanol 9:1, v/v) and recrystallized in heptane or acetonitrile (except for compound **30**) to afford the titled compounds (**11** and **17−40**).

***N*3-(1-Adamantyl)-6-methyl-1-pentyl-4-oxo-1,4-dihydropyridine-3-carboxamide (11).** Beige solid (57%); mp 195 °C. ^{1}H NMR ($CDCl_3$) δ 10.15 (s, 1H), 8.38 (s, 1H), 6.38 (s, 1H), 3.86 (t, 2H, J = 7.8 Hz), 2.35 (s, 3H), 2.14 (m, 9H), 1.71 (m, 8H), 1.34 (m, 4H), 0.92 (t, 3H, J = 6.9 Hz). LC-MS (APCI$^+$) m/z 357.4 (MH$^+$).

***N*3-(1-Adamantyl)-6-*tert*-butyl-1-pentyl-4-oxo-1,4-dihydropyridine-3-carboxamide (17).** Beige solid (49%); mp 72 °C. ^{1}H NMR ($CDCl_3$) δ 10.07 (s, 1H), 8.39 (s, 1H), 6.58 (s, 1H), 4.06 (t, 2H, J = 8.3 Hz), 2.14 (m, 9H), 1.71 (m, 8H), 1.42 (s, 9H), 1.36 (m, 4H), 0.93 (t, 3H, J = 6.6 Hz). LC-MS (APCI$^+$) m/z 399.3 (MH$^+$).

***N*3-(Cyclohexyl)-6-*tert*-butyl-1-pentyl-4-oxo-1,4-dihydropyridine-3-carboxamide (18).** Beige solid (53%); mp 91 °C. ^{1}H NMR ($CDCl_3$) δ 10.2 (d, 1H, J = 7.3 Hz), 8.40 (s, 1H), 6.58 (s, 1H), 4.08 (t, 2H, J = 8.3 Hz), 3.96 (m, 1H), 1.94−1.73 (m, 7H), 1.43−1.37 (m, 18H), 0.93 (t, 3H, J = 6.6 Hz). LC-MS (APCI$^+$) m/z 347.2 (MH$^+$).

(*R*,*S*)-*N*3-(1-(1-Adamantyl)ethyl)-1-ethyl-4-oxo-6-phenyl-1,4-dihydropyridine-3-carboxamide (19). Beige solid (54%); mp 224 °C. ^{1}H NMR ($CDCl_3$) δ 10.41 (d, 1H, J = 9.1 Hz), 8.58 (s, 1H), 7.53 (m, 3H), 7.35 (m, 2H), 6.47 (s, 1H), 3.87 (m, 3H), 2.00 (m, 3H), 1.64 (m, 12H), 1.25 (t, 3H, J = 7.3 Hz), 1.13 (d, 3H, J = 7.0 Hz). LC-MS (APCI$^+$) m/z 405.1 (MH$^+$).

(*R*,*S*)-*N*3-(1-(1-Adamantyl)ethyl)-4-oxo-1-pentyl-6-phenyl-1,4-dihydropyridine-3-carboxamide (20). White solid (52%); mp 169 °C. ^{1}H NMR ($CDCl_3$) δ 10.41 (d, 1H, J = 9.1 Hz), 8.55 (s, 1H), 7.52 (m, 3H), 7.33 (m, 2H), 6.47 (s, 1H), 3.91 (m, 1H), 3.79 (t, 2H, J = 7.7 Hz), 2.00 (m, 3H), 1.64 (m, 14H), 1.15 (m, 7H), 0.79 (t, 3H, J = 6.9 Hz). LC-MS (APCI$^+$) m/z 447.4 (MH$^+$).

(*R*,*S*)-*N*3-(1-(1-Adamantyl)ethyl)-1,6-diphenyl-4-oxo-1,4-dihydropyridine-3-carboxamide (21). White solid (47%); mp > 250 °C. ^{1}H NMR ($CDCl_3$) δ 10.35 (d, 1H, J = 9.1 Hz), 8.70 (s, 1H), 7.32 (m, 6H), 7.10 (m, 4H), 6.86 (s, 1H), 3.90 (m, 1H), 2.00 (m, 3H), 1.69 (m, 12H), 1.17 (d, 3H, J = 6.7 Hz). LC-MS (APCI$^+$) m/z 453.4 (MH$^+$).

***N*3-((1-Adamantyl)methyl)-4-oxo-1-pentyl-6-phenyl-1,4-dihydropyridine-3-carboxamide (22).** White solid (57%); mp 154 °C. ^{1}H NMR ($CDCl_3$) δ 10.39 (m, 1H), 8.56 (s, 1H), 7.51 (m, 3H), 7.35 (m, 2H), 6.47 (s, 1H), 3.79 (t, 2H, J = 7.7 Hz), 3.16 (d, 2H, J = 6.1 Hz), 1.99 (m, 3H), 1.69−1.61 (m, 14H), 1.12 (m, 4H), 0.78 (t, 3H, J = 6.9 Hz). LC-MS (APCI$^+$) m/z 433.3 (MH$^+$).

***N*3-(1-(3,5-Dimethyl)adamantyl)-4-oxo-1-pentyl-6-phenyl-1,4-dihydropyridine-3-carboxamide (23).** White solid (62%); mp 133 °C. ^{1}H NMR ($CDCl_3$) δ 10.21 (s, 1H), 8.5 (s, 1H), 7.5−7.35 (m, 5H), 6.45 (s, 1H), 3.77 (t, 2H, J = 7.1 Hz), 2.00−1.18 (m, 19H), 0.88 (s, 6H), 0.79 (t, 3H, J = 7.0 Hz). LC-MS (APCI$^+$) m/z 447.3 (MH$^+$).

***N*3-(1-Adamantyl)-1-butyl-4-oxo-6-phenyl-1,4-dihydropyridine-3-carboxamide (24).** White solid (30%); mp 146 °C. ^{1}H NMR (DMSO-d_6) δ 10.19 (s, 1H), 8.53 (s, 1H), 7.53 (m, 5H), 6.25 (s, 1H), 3.90 (t, 2H, J = 7.4 Hz), 2.03 (m, 9H), 1.66 (m, 6H), 1.40 (m, 2H), 1.04 (m, 2H), 0.65 (t, 3H, J = 7.3 Hz). LC-MS (APCI$^+$) m/z 405.2 (MH$^+$).

***N*3-(1-Adamantyl)-4-oxo-1-pentyl-6-phenyl-1,4-dihydropyridine-3-carboxamide (25).** Beige solid (55%); mp 145 °C. ^{1}H NMR ($CDCl_3$) δ 10.17 (s, 1H), 8.51 (s, 1H), 7.51 (m, 3H), 7.34 (m, 2H), 6.45 (s, 1H), 3.77 (t, 2H, J = 7.7 Hz), 2.16 (m, 9H), 1.72−1.58 (m, 8H), 1.12 (m, 4H), 0.81 (t, 3H, J = 6.9 Hz). LC-MS (APCI$^+$) m/z 419.3 (MH$^+$).

***N*3-(1-Adamantyl)-1-hexyl-4-oxo-6-phenyl-1,4-dihydropyridine-3-carboxamide (26).** White solid (32%); mp 167 °C. ^{1}H NMR (DMSO-d_6) δ 10.19 (s, 1H), 8.53 (s, 1H), 7.54 (m, 5H), 6.25 (s, 1H), 3.90 (t, 2H, J = 7.6 Hz), 2.03 (m, 9H), 1.66 (m, 6H), 1.41 (m, 2H), 1.00 (m, 6H), 0.74 (t, 3H, J = 7.0 Hz). LC-MS (APCI$^+$) m/z 433.3 (MH$^+$).

***N*3-(Cyclohexyl)-4-oxo-1-pentyl-6-phenyl-1,4-dihydropyridine-3-carboxamide (27).** White solid (64%); mp 120 °C. ^{1}H NMR ($CDCl_3$) δ 10.31 (d, 1H, J = 7.6 Hz), 8.54 (s, 1H), 7.52 (m, 3H), 7.35 (m, 2H), 6.46 (s, 1H), 4.00 (m, 1H), 3.80 (t, 2H, J = 7.7 Hz),

1.98−1.12 (m, 16H), 0.79 (t, 3H, J = 6.9 Hz). LC-MS (APCI$^+$) m/z 366.2 (MH$^+$).

(*R*)-4-Oxo-1-pentyl-6-phenyl-*N*3-(1-(1,2,3,4-tetrahydronaphthyl))-1,4-dihydropyridine-3-carboxamide (28). To obtain compound **28**, the pure enantiomer, (*R*)-1,2,3,4-tetrahydro-1-naphthylamine was used. White solid (60%); mp 139 °C. ^{1}H NMR ($CDCl_3$) δ 10.66 (d, 1H, J = 8.2 Hz), 8.61 (s, 1H), 7.52 (m, 3H), 7.35 (m, 3H), 7.13 (m, 3H), 6.44 (s, 1H), 5.45 (m, 1H), 3.81 (t, 2H, J = 7.7 Hz), 2.86 (m, 2H), 1.97 (m, 2H), 1.57 (m, 4H), 1.44−1.28 (m, 4H), 0.8 (t, 3H, J = 7.0 Hz). LC-MS (APCI$^+$) m/z 415.3 (MH$^+$).

(*S*)-4-Oxo-1-pentyl-6-phenyl-*N*3-(1-(1,2,3,4-tetrahydronaphthyl))-1,4-dihydropyridine-3-carboxamide (29). To obtain compound **29**, the pure enantiomer, (*S*)-1,2,3,4-tetrahydro-1-naphthylamine was used. White solid (52%); mp 139 °C. ^{1}H NMR ($CDCl_3$) and LC-MS (APCI$^+$) (see compound **28**).

4-Oxo-1-pentyl-6-phenyl-*N*3-(piperidin-1-yl)-1,4-dihydropyridine-3-carboxamide (30). White powder (40%); mp 122 °C. ^{1}H NMR ($CDCl_3$) δ 11.17 (s, 1H), 8.56 (s, 1H), 7.53 (m, 3H), 7.33 (m, 2H), 6.48 (s, 1H), 3.81 (t, 2H, J = 7.6 Hz), 2.92 (t, 4H, J = 5.1 Hz), 1.77−1.48 (m, 8H), 1.12 (m, 4H), 0.79 (t, 3H, J = 6.9 Hz). LC-MS (APCI$^+$) m/z 368.3 (MH$^+$).

4-Oxo-1-pentyl-6-phenyl-*N*3-(3(trifluoromethyl)phenyl)-1,4-dihydropyridine-3-carboxamide (31). White solid (74%); mp 125 °C. ^{1}H NMR ($CDCl_3$) δ 12.80 (s, 1H), 8.64 (s, 1H), 8.18 (s, 1H), 7.89 (d, 1H, J = 7.6 Hz), 7.54−7.37 (m, 7H), 6.56 (s, 1H), 3.86 (t, 2H, J = 7.7 Hz), 1.64 (m, 2H), 1.14 (m, 4H), 0.8 (t, 3H, J = 6.7 Hz). LC-MS (APCI$^+$) m/z 429.6 (MH$^+$).

***N*3-(1-Adamantyl)-6-(4-chlorophenyl)-1-pentyl-4-oxo-1,4-dihydropyridine-3-carboxamide (32).** White powder (28%); mp 190 °C. ^{1}H NMR (DMSO-d_6) δ 10.17 (s, 1H), 8.53 (s, 1H), 7.61 (d, 2H, J = 8.7 Hz), 7.55 (d, 2H, J = 8.7 Hz), 6.27 (s, 1H), 3.9 (t, 2H, J = 7.6 Hz), 2.03 (m, 9H), 1.66 (m, 6H), 1.42 (m, 2H), 1.05 (m, 4H), 0.71 (t, 3H, J = 6.8 Hz). LC-MS (APCI$^+$) m/z 453.3 (MH$^+$).

6-(4-Chlorophenyl)-*N*3-cyclohexyl-4-oxo-1-pentyl-1,4-dihydropyridine-3-carboxamide (33). White powder (32%); mp 157 °C. ^{1}H NMR ($CDCl_3$) δ 10.31 (d, 1H, J = 7.9 Hz), 8.58 (s, 1H), 7.61 (d, 2H, J = 8.7 Hz), 7.55 (d, 2H, J = 8.7 Hz), 6.29 (s, 1H), 3.92 (t, 2H, J = 7.6 Hz), 3.82 (m, 1H) 1.83−1.31 (m, 12H), 1.03 (m, 4H), 0.71 (t, 3H, J = 6.8 Hz). LC-MS (APCI$^+$) m/z 401.3 (MH$^+$).

6-(4-Chlorophenyl)-4-oxo-1-pentyl-*N*3-(3(trifluoromethyl)phenyl)-1,4-dihydropyridine-3-carboxamide (34). White powder (38%); mp 100 °C. ^{1}H NMR ($CDCl_3$) δ 13.03 (s, 1H), 8.80 (s, 1H), 8.29 (s, 1H), 7.78 (d, 2H, J = 8.1 Hz), 7.63 (m, 3H), 7.45 (d, 2H, J = 7.6 Hz), 6.46 (s, 1H), 3.99 (t, 2H, J = 7.4 Hz), 1.45 (m, 2H), 1.06 (m, 4H), 0.72 (t, 3H, J = 6.8 Hz). LC-MS (APCI$^+$) m/z 463.2 (MH$^+$).

***N*3-(1-Adamantyl)-6-(3-chlorophenyl)-1-pentyl-4-oxo-1,4-dihydropyridine-3-carboxamide (35).** Beige solid (62%); mp 178 °C. ^{1}H NMR ($CDCl_3$) δ 10.10 (s, 1H), 8.50 (s, 1H), 7.49 (m, 2H), 7.34 (s, 1H), 7.24 (d, 2H, J = 7.6 Hz), 6.42 (s, 1H), 3.75 (t, 2H, J = 7.6 Hz), 2.15 (m, 9H), 1.70 (m, 8H), 1.13 (m, 4H), 0.80 (t, 3H, J = 6.8 Hz). LC-MS (APCI$^+$) m/z 453.2 (MH$^+$).

***N*3-(1-Adamantyl)-6-(2-chlorophenyl)-1-pentyl-4-oxo-1,4-dihydropyridine-3-carboxamide (36).** White solid (58%); mp 166 °C. ^{1}H NMR ($CDCl_3$) δ 10.15 (s, 1H), 8.54 (s, 1H), 7.50 (m, 4H), 6.42 (s, 1H), 3.66 (t, 2H, J = 7.6 Hz), 2.16 (m, 9H), 1.70 (m, 8H), 1.11 (m, 4H), 0.79 (t, 3H, J = 6.8 Hz). LC-MS (APCI$^+$) m/z 453.2 (MH$^+$).

***N*3-(1-Adamantyl)-6-(4-methylphenyl)-1-pentyl-4-oxo-1,4-dihydropyridine-3-carboxamide (37).** White solid (73%); mp 210 °C. ^{1}H NMR ($CDCl_3$) δ 10.19 (s, 1H), 8.50 (s, 1H), 7.30 (d, 2H, J = 8.4 Hz), 7.22 (d, 2H, J = 8.1 Hz), 6.43 (s, 1H), 3.78 (t, 2H, J = 7.6 Hz), 2.43 (s, 3H) 2.16 (m, 9H), 1.72 (m, 6H), 1.58 (m, 2H), 1.13 (m, 4H), 0.79 (t, 3H, J = 6.8 Hz). LC-MS (APCI$^+$) m/z 433.3 (MH$^+$).

***N*3-(1-Adamantyl)-6-(4-methoxyphenyl)-1-pentyl-4-oxo-1,4-dihydropyridine-3-carboxamide (38).** White solid (73%); mp 144 °C. ^{1}H NMR ($CDCl_3$) δ 10.19 (s, 1H), 8.50 (s, 1H), 7.24 (d, 2H, J = 8.7 Hz), 7.01 (d, 2H, J = 8.7 Hz), 6.43 (s, 1H), 3.88 (s, 3H) 3.79 (t, 2H, J = 7.6 Hz), 2.16 (m, 9H), 1.70 (m, 8H), 1.14 (m, 4H), 0.80 (t, 3H, J = 6.8 Hz). LC-MS (APCI$^+$) m/z 449.3 (MH$^+$).

***N*3-(1-Adamantyl)-1-pentyl-6-phenyl-4-thioxo-1,4-dihydropyridine-3-carboxamide (39).** Yellow solid (56%); mp 163 °C. ^{1}H NMR ($CDCl_3$) δ 11.41 (s, 1H), 8.75 (s, 1H), 7.60 (s, 1H), 7.54 (m, 3H), 7.34 (m, 2H), 3.88 (t, 2H, J = 7.7 Hz), 2.22 (m, 9H), 1.75−1.56 (m, 8H), 1.13 (m, 4H), 0.79 (t, 3H, J = 7.0 Hz). LC-MS (APCI$^+$) m/z 435.3 (MH$^+$).

***N*3-(Cyclohexyl)-1-pentyl-6-phenyl-4-thioxo-1,4-dihydropyridine-3-carboxamide (40).** Yellow solid (59%); mp 119 °C. ^{1}H NMR ($CDCl_3$) δ 11.53 (d, 1H, J = 7.3 Hz), 8.76 (s, 1H), 7.60 (s, 1H), 7.53 (m, 3H), 7.35 (m, 2H), 4.09 (m, 1H), 3.91 (t, 2H, J = 7.7 Hz), 1.97 (m, 2H), 1.80−1.59 (m, 10H), 1.13 (m, 4H), 0.82 (t, 3H, J = 6.8 Hz). LC-MS (APCI$^+$) m/z 383.3 (MH$^+$).

***tert*-Butyl 4-Oxo-1-pentyl-6-phenyl-1,4-dihydropyridin-3-yl carbamate (41).** To a solution of carboxylic acid **16d** (0.4 g, 1.4 mmol) in *tert*-butyl alcohol (20 mL) were added under nitrogen atmosphere, potassium *tert*-butoxide (0.17 g, 1.7 mmol) and diphenylphosphoryl azide (0.36 mL, 1.7 mmol). The mixture was refluxed for 12 h, cooled to room temperature, and diluted with EtOAc. The organic phase was washed with saturated aqueous $NaHCO_3$ solution and brine, dried over $MgSO_4$, and concentrated under reduced pressure to a yellowish oil. The latter was purified by silica gel chromatography (dichloromethane/methanol 95:5, v/v) to afford pure **41** (0.17 g, 38%) as a yellow oil. ^{1}H NMR (DMSO-d_6) δ 8.39 (s, 1H), 7.74 (s, 1H), 7.56−7.43 (m, 5H), 6.12 (s, 1H), 3.81 (t, 2H, J = 7.6 Hz), 1.48 (m, 11H), 1.03 (m, 4H), 0.69 (t, 3H, J = 6.8 Hz). LC-MS (APCI$^+$) m/z 357.1 (MH$^+$).

5-Amino-1-pentyl-2-phenyl-1*H*-pyridin-4-one (42). To a solution of 5N hydrochloric acid in isopropyl alcohol (20 mL) was added the carbamate **41** (0.1 g, 0.28 mmol). The mixture was stirred at room temperature for 14 h and then concentrated under reduced pressure. The resulting solid was solubilized in water and washed with Et_2O. The aqueous phase was alkalinized with 10% NaOH and extracted with EtOAc. The organic phase was dried over $MgSO_4$ and the solvent removed under reduced pressure to afford pure **42** as a white solid (0.068 g, 95%); mp 98 °C. ^{1}H NMR (DMSO-d_6) δ 7.48−7.38 (m, 5H), 7.19 (s, 1H), 5.82 (s, 1H), 4.67 (s, 2H), 3.67 (t, 2H, J = 7.3 Hz), 1.46 (m, 2H), 1.04 (m, 4H), 0.72 (t, 3H, J = 6.7 Hz). LC-MS (APCI$^+$) m/z 257.1 (MH$^+$).

***N*-(4-Oxo-1-pentyl-6-phenyl-1,4-dihydropyridin-3-yl)cyclohexanecarboxamide (43).** Compound **43** was obtained using the same procedure described for amides **11** and **17**−**40**. Purification by silica gel chromatography (ethyl acetate/cyclohexane 1:1); white solid (38%); mp 179 °C. ^{1}H NMR ($CDCl_3$) δ 8.94 (s, 1H), 8.57 (s, 1H), 7.48 (m, 3H), 7.33 (m, 2H), 6.37 (s, 1H), 3.72 (t, 2H, J = 7.9 Hz), 2.37 (m, 1H), 2.00−1.11 (m, 16H), 0.91 (t, 3H, J = 7.0 Hz). LC-MS (APCI$^+$) m/z 367.3 (MH$^+$).

Pharmacology. *h*CB_1 and *h*CB_2 membranes of CHO cells were purchased from PerkinElmer. Fatty acid free bovine serum albumin (BSA) was purchased from Sigma Chemical Co. (St. Louis, MO). WIN-55,212-2 was purchased from RBI (Natick, MA), HU-210 and CP-55,940 from Tocris (Bristol, UK), and SR141716A and **5** were kindly donated by Sanofi Recherche (Montpellier, France). [^{3}H]-SR141716A (52 Ci/mol) was from Amersham (Roosendaal, The Netherlands), [^{3}H]-CP-55,940 (101 Ci/mol) was from NEN Life Science (Zaventem, Belgium), and HU-210 was from Tocris (Bristol, UK). Glass fiber filters were purchased from Whatman (Maidstone, UK), while Aqualuma was from PerkinElmer (Schaesberg, The Netherlands). [^{35}S]-GTPγS (1173 Ci/mmol) was from Amersham (Roosendaal, The Netherlands).

Competition Binding Assay. Stock solutions of the compounds were prepared in DMSO and further diluted (100×) with the binding buffer to the desired concentration. Final DMSO concentrations in the assay were less than 0.1%. The

competitive binding experiments were performed as described earlier.[57] Briefly [^{3}H]-SR141716A (1 nM) or [^{3}H]-CP-55,940 (1nM) as radioligands for the hCB$_1$ and the hCB$_2$ cannabinoid receptor, respectively, were added to 40 μg of membranes resuspended in 0.5 mL (final volume) binding buffer (50 mM Tris-HCl, 3 mM $MgCl_2$, 1 mM EDTA, 0.5% bovine serum albumine, pH 7.4). After 1 h at 30 °C, the incubation was stopped and the solutions were rapidly filtered through 0.5% PEI pretreated GF/B glass fiber filters on a M-48T Brandell cell harvester and washed twice with 5 mL of ice-cold binding buffer without serum albumin. The radioactivity on the filters was measured using a Pharmacia Wallac 1410 β-counter using 10 mL of Aqualuma, after 10 s shaking and 3 h resting. Assays were performed at least in triplicate. The nonspecific binding was determined in the presence of 10 μM HU-210.

[^{35}S]-GTPγS Assays. The binding experiments were performed at 30 °C in tubes containing 40 μg protein in 0.5 mL (final volume) binding buffer (50 mM Tris-HCl, 3 mM $MgCl_2$, 1 mM EDTA, 100 mM NaCl, 0.1% bovine serum albumin, pH 7.4) supplemented with 20 μM GDP. The assay was initiated by the addition of [^{35}S]-GTPγS (0.05 nM, final concentration). After 1 h, the incubations were terminated by the addition of 5 mL of ice-cold washing buffer (50 mM Tris-HCl, 3 mM $MgCl_2$, 1 mM EDTA, 100 mM NaCl). The suspension was immediately filtered through GF/B filters using a 48 well Brandell cell harvester and washed twice with the same ice-cold buffer. The radioactivity on the filters was counted as mentioned above. Assays were performed in triplicate. The nonspecific binding was measured in the presence of 100 μM Gpp(NH)p. Results were expressed as EC_{50} (nM) and E_{max} (%). Basal constitutive activity of the receptor has been set at a value of 100%; reported E_{max} values above 100% indicated that the compound behaves as an agonist (either partial or full), values under 100% indicated inverse agonist properties.

Data Analysis. IC_{50} and EC_{50} values were determined by nonlinear regression analysis performed using the GraphPad prism 4.0 program (GraphPad Software, San Diego). The K_i values were calculated from the IC_{50}, based on the Cheng−Prusoff equation: $Ki = IC_{50}/(1 + L/K_d)$. Statistical signification of [^{35}S]-GTPγS assay results was assessed using a one-way ANOVA followed by a Dunett post-test.

Homology Modeling of the Inactive Human CB$_2$ Apo-Receptor. Sequence homology rates are very comparable between each GPCR crystal and CB$_2$ sequences (44%, 46%, 44%, and 46% in conserved pattern and 40%, 37%, 37%, and 39% in whole sequences in bovine rhodopsin, turkey β1-adrenergic receptor, human β2-adrenergic receptor, and A2A adenosine receptor, respectively). However, the two serine residues 4.53 (161) and 4.57 (165), known as critical for the binding of **5**,[58] were simultaneously conserved only in the sequences of the β-adrenergic receptors. The human β2-adrenergic receptor (PDB 2RH1) was selected as the crystal template for homology modeling because it has the advantage of conserving the tyrosine residue in position 5.58 (209) of the critical TM V instead of an alanine residue in the sequence of the turkey β1-adrenergic receptor. Indeed, CB$_1$ and CB$_2$ receptors lack the highly conserved residue Pro5.50 in the class A GPCRs. Thus the second most highly conserved residue, Tyr5.58, has been described as the new reference amino acid in TM V concerning CB$_1$ and CB$_2$ receptors.[59,60]

The input sequence alignment for homology modeling by MODELER software[61] was automatically generated by ClustalW,[62] taking care to shift gaps out from the transmembrane regions. Then the insertion/deletion gaps were manually adjusted in loop regions, which are generated without any homology restraint by a simulated annealing procedure included in the MODELER program. Thus the one-residue gaps in IL1 (insertion), EL1 (deletion), and EL3 (insertion) were moved to the center of the loops so that no bulky or misfolded peptide is introduced in regions flanking transmembrane helices. Further attention was given to the EL2 region, which is very variable among GPCRs and known to be critical for ligand binding.[63−65] The compact structural folding of the template loop was conserved by adjusting the 10 gap deletions in the N-terminal moiety of the loop. Contrary to the unstructured C-terminal moiety of EL2 region in the β2-adrenergic receptor, the N-terminal segment is structured as an α-helix and could keep reliable Cα−Cα restraints editing deletion gaps in this region (see Figure 1). The intracellular lopp (IL) 3 region was also fully automatically generated as previously described because this loop is lacking in the crystal template, whereas the N-terminal (Met1-Leu28) and C-terminal (His316-Cys360) overhangs that are not aligned to the template sequence were not modeled. The homology process was carried out on the basis of the input sequence alignment as well as spatial restraints applied for the highly potential disulfide bridge between Cys174 and Cys179.

An energy minimization of hydrogens and side chains was then performed using the CHARMM forcefield[66] and processing 5000 steps with the steepest descent algorithm converging to a 0.1 kcal·mol^{-1}·Å^{-1} gradient, followed by 20000 steps with the conjugate gradient, converging to a 0.001 kcal·mol^{-1}·Å^{-1} gradient. Graphical inspection of models was performed using the Sybyl 6.9.2 software (Tripos Associates, Inc., 1699 South Hanley Road, St. Louis, MO 63144).

Modeling Ligand-Bound States of the CB$_2$ Receptor Model with Both Compounds 17 and 25. After the identification of the putative binding site using the MOLCAD program of Sybyl 6.9.2, both compounds **17** and **25** were therein submitted docking routines using GOLDv4.1.1 software[67] in a 8 Å sphere including the entire solvent-accessible surface. For each ligand, 30 preferential conformations were calculated and ranked following the goldscore fitness scoring function. An early termination was allowed as three top-ranked solutions were within a 1.5 Å RMSd. Once the most relevant docking solution was chosen for each ligand, both receptor−ligand complexes underwent a CHARMM energy minimization as previously described in order to discard steric clashes. Finally, both complexes were submitted to a 10 ns molecular dynamics (MD) CHARMM simulation applying harmonic restraints on the TM bundle backbone and a distance−dependent dielectrics arguing for an implicit representation of solvent in outer regions. During the MD simulation, the binding energy was monitored in each receptor−ligand complex following the formula: $\Delta G_{binding} = \Delta G_{complex} - \Delta G_{ligand} - \Delta G_{protein}$.

Acknowledgment. This work was financially supported by a grant from the Nord-Pas-de-Calais Regional Council and University of Lille 2.

References

(1) De Petrocellis, L.; Cascio, M. G.; Di Marzo, V. The Endocannabinoid System: A General View and Latest Additions. *Br. J. Pharmacol.* **2004**, *141*, 765–774.
(2) Howlett, A. C.; Barth, F.; Bonner, T. I.; Cabral, G.; Casellas, P.; Devane, W. A.; Felder, C. C.; Herkenham, M.; Mackie, K.; Martin, B. R.; Mechoulam, R.; Pertwee, R. G. International Union of Pharmacology. XXVII. Classification of Cannabinoid Receptors. *Pharmacol. Rev.* **2002**, *54*, 161–202.
(3) Lambert, D. M.; Fowler, C. J. The Endocannabinoid System: Drug Targets, Lead Compounds, and Potential Therapeutic Applications. *J. Med. Chem.* **2005**, *48*, 5059–5087.
(4) Pacher, P.; Bátkai, S.; Kunos, G. The Endocannabinoid System as an Emerging Target of Pharmacotherapy. *Pharmacol. Rev.* **2006**, *58*, 389–462.
(5) Compton, D. R.; Rice, K. C.; De Costa, B. R.; Razdan, R. K.; Melvin, L. S.; Johnson, M. R.; Martin, B. R. Cannabinoid Structure−Activity Relationships: Correlation of Receptor Binding and in Vivo Activities. *J. Pharmacol. Exp. Ther.* **1993**, *265*, 218–226.
(6) Malan, T. P., Jr.; Ibrahim, M. M.; Lai, J.; Vanderah, T. W.; Makriyannis, A.; Porreca, F. CB$_2$ Cannabinoid Receptor Agonists: Pain Relief Without Psychoactive Effects? *Curr. Opin. Pharmacol.* **2003**, *3*, 62–67.

(7) Galiègue, S.; Mary, S.; Marchand, J.; Dussossoy, D.; Carrière, D.; Carayon, P.; Bouaboula, M.; Shire, D.; Le Fur, G.; Casellas, P. Expression of Central and Peripheral Cannabinoid Receptors in Human Immune Tissues and Leukocyte Subpopulations. *Eur. J. Biochem.* **1995**, *232*, 54–61.

(8) Van Sickle, M. D.; Duncan, M.; Kingsley, P. J.; Mouihate, A.; Urbani, P.; Mackie, K.; Stella, N.; Makriyannis, A.; Piomelli, D.; Davison, J. S.; Marnett, L. J.; Di Marzo, V.; Pittman, Q. J.; Patel, K. D.; Sharkey, K. A. Identification and Functional Characterization of Brainstem Cannabinoid CB_2 receptors. *Science* **2005**, *310*, 329–332.

(9) Fernández-Ruiz, J.; Romero, J.; Velasco, G.; Tolón, R. M.; Ramos, J. A.; Guzmán, M. Cannabinoid CB_2 Receptor: A New Target for Controlling Neural Cell Survival? *Trends Pharmacol. Sci.* **2007**, *28*, 39–45.

(10) Wright, K.; Rooney, N.; Feeney, M.; Tate, J.; Robertson, D.; Welham, M.; Ward, S. Differential Expression of Cannabinoid Receptors in the Human Colon: Cannabinoids Promote Epithelial Wound Healing. *Gastroenterology* **2005**, *129*, 437–453.

(11) Mukhopadhyay, S.; Das, S.; Williams, E. A.; Moore, D.; Jones, J. D.; Zahm, D. S.; Ndengele, M. M.; Lechner, A. J.; Howlett, A. C. Lipopolysaccharide and Cyclic AMP Regulation of CB_2 Cannabinoid Receptor Levels in Rat Brain and Mouse RAW 264.7 Macrophages. *J. Neuroimmunol.* **2006**, *181*, 82–92.

(12) Buckley, N. E.; McCoy, K. L.; Mezey, E.; Bonner, T.; Zimmer, A.; Felder, C. C.; Glass, M.; Zimmer, A. Immunomodulation by Cannabinoids is Absent in Mice Deficient for the Cannabinoid CB_2 receptor. *Eur. J. Pharmacol.* **2000**, *396*, 141–149.

(13) Klegeris, A.; Bissonnette, C. J.; McGeer, P. L. Reduction of Human Monocytic Cell Neurotoxicity and Cytokine Secretion by Ligands of the Cannabinoid-Type CB_2 Receptor. *Br. J. Pharmacol.* **2003**, *139*, 775–786.

(14) Ihenetu, K.; Molleman, A.; Parsons, M. E.; Whelan, C. J. Inhibition of Interleukin-8 Release in the Human Colonic Epithelial Cell Line HT-29 by Cannabinoids. *Eur. J. Pharmacol.* **2003**, *458*, 207–215.

(15) Jordà, M. A.; Verbakel, S. E.; Valk, P. J.; Vankan-Berkhoudt, Y. V; Maccarrone, M.; Finazzi-Agrò, A.; Löwenberg, B.; Delwel, R. Hematopoietic Cells Expressing the Peripheral Cannabinoid Receptor Migrate in Response to the Endocannabinoid 2-Arachidonoylglycerol. *Blood* **2002**, *99*, 2786–2793.

(16) Kishimoto, S.; Gokoh, M.; Oka, S.; Muramatsu, M.; Kajiwara, T.; Waku, K.; Sugiura, T. 2-Arachidonoylglycerol Induces the Migration of HL-60 Cells Differentiated into Macrophage-Like Cells and Human Peripheral Blood Monocytes Through the Cannabinoid CB_2 Receptor-Dependent Mechanism. *J. Biol. Chem.* **2003**, *278*, 24469–24475.

(17) Miller, A. M.; Stella, N. CB_2 Receptor-Mediated Migration of Immune Cells: It Can Go Either Way. *Br. J. Pharmacol.* **2008**, *153*, 299–308.

(18) Ramirez, B. G.; Blazquez, C.; Gomez del Pulgar, T.; Guzman, M.; de Ceballos, M. L. Prevention of Alzheimer's Disease Pathology by Cannabinoids: Neuroprotection Mediated by Blockade of Microglial Activation. *J. Neurosci.* **2005**, *25*, 1904–1913.

(19) Kimball, E. S.; Schneider, C. R.; Wallace, N. H.; Hornby, P. J. Agonists of Cannabinoid Receptor 1 and 2 Inhibit Experimental Colitis Induced by Oil of Mustard and by Dextran Sulfate Sodium. *Am. J. Physiol.: Gastrointest. Liver Physiol.* **2006**, *291*, G364–G371.

(20) Wright, K. L.; Duncan, M.; Sharkey, K. A. Cannabinoid CB_2 receptors in the gastrointestinal tract: a regulatory system in states of inflammation. *Br. J. Pharmacol.* **2008**, *153*, 263–270.

(21) Body-Malapel, M.; El Bakali, J.; Mérour, E.; Stern, E.; Millet, R.; Desreumaux, P. 4-Oxo-1,4-dihydroquinoline-3-carboxamides Derivatives as New Potent and Selective CB_2 Agonists with Anti-inflammatory and Analgesic Properties in the Gut. *Gastroenterology* **2008**, *134*, A–107.

(22) Docagne, F.; Muñetón, V.; Clemente, D.; Ali, C.; Loría, F.; Correa, F.; Hernangómez, M.; Mestre, L.; Vivien, D.; Guaza, C. Excitotoxicity in a Chronic Model of Multiple Sclerosis: Neuroprotective Effects of Cannabinoids Through CB_1 and CB_2 Receptor Activation. *Mol. Cell. Neurosci.* **2007**, *34*, 551–561.

(23) Benito, C.; Romero, J. P.; Tolón, R. M.; Clemente, D.; Docagne, F.; Hillard, C. J.; Guaza, C.; Romero, J. Cannabinoid CB_1 and CB_2 Receptors and Fatty Acid Amide Hydrolase are Specific Markers of Plaque Cell Subtypes in Human Multiple Sclerosis. *J. Neurosci.* **2007**, *27*, 2396–2402.

(24) Yao, B. B.; Hsieh, G. C.; Frost, J. M.; Fan, Y.; Garrison, T. R.; Daza, A. V.; Grayson, G. K.; Zhu, C. Z.; Pai, M.; Chandran, P.; Salyers, A. K; Wensink, E. J.; Honore, P.; Sullivan, J. P.; Dart, M. J.; Meyer, M. D. In Vitro and in Vivo Characterization of A-796260: A Selective Cannabinoid CB_2 Receptor Agonist Exhibiting Analgesic Activity in Rodent Pain Models. *Br. J. Pharmacol.* **2008**, *153*, 390–401.

(25) Ofek, O.; Karsak, M.; Leclerc, N.; Fogel, M.; Frenkel, B.; Wright, K.; Tam, J.; Attar-Namdar, M.; Kram, V.; Shohami, E.; Mechoulam, R.; Zimmer, A.; Bab, I. Peripheral Cannabinoid Receptor, CB_2, Regulates Bone Mass. *Proc. Natl. Acad. Sci. U.S.A.* **2006**, *103*, 696–701.

(26) Frost, J. M.; Dart, M. J.; Tietje, K. R.; Garrison, T. R.; Grayson, G. K.; Daza, A. V.; El-Kouhen, O. F.; Miller, L. N.; Li, L.; Yao, B. B.; Hsieh, G. C.; Pai, M.; Zhu, C. Z.; Chandran, P.; Meyer, M. D. Indol-3-yl-tetramethylcyclopropyl Ketones: Effects of Indole Ring Substitution on CB_2 Cannabinoid Receptor Activity. *J. Med. Chem.* **2008**, *51*, 1904–1912.

(27) Huffman, J. W.; Liddle, J.; Yu, S.; Aung, M. M.; Abood, M. E.; Wiley, J. L.; Martin, B. R. 3-(1′,1′-Dimethylbutyl)-1-deoxy-delta^8-THC and Related Compounds: Synthesis of Selective Ligands for the CB_2 Receptor. *Bioorg. Med. Chem.* **1999**, *7*, 2905–2914.

(28) Poso, A.; Huffman, J. W. Targeting the Cannabinoid CB_2 Receptor: Modelling and Structural Determinants of CB_2 Selective Ligands. *Br. J. Pharmacol.* **2008**, *153*, 335–346.

(29) Ohta, H.; Ishizaka, T.; Tatsuzuki, M.; Yoshinaga, M.; Iida, I.; Yamaguchi, T.; Tomishima, Y.; Futaki, N.; Toda, Y.; Saito, S. Imine Derivatives as New Potent and Selective CB_2 Cannabinoid Receptor Agonists with an Analgesic Action. *Bioorg. Med. Chem.* **2008**, *16*, 1111–1124.

(30) Giblin, G. M.; O'Shaughnessy, C. T.; Naylor, A.; Mitchell, W. L.; Eatherton, A. J.; Slingsby, B. P.; Rawlings, D. A.; Goldsmith, P.; Brown, A. J.; Haslam, C. P.; Clayton, N. M.; Wilson, A. W.; Chessell, I. P.; Wittington, A. R.; Green, R. Discovery of 2-[(2,4-Dichlorophenyl)amino]-*N*-[(tetrahydro-*2H*-pyran-4-yl)methyl]-4-(trifluoromethyl)-5-pyrimidinecarboxamide, a Selective CB_2 Receptor Agonist for the Treatment of Inflammatory Pain. *J. Med. Chem.* **2007**, *50*, 2597–2600.

(31) Rinaldi-Carmona, M.; Barth, F.; Millan, J.; Derocq, J. M.; Casellas, P.; Congy, C.; Oustric, D.; Sarran, M.; Bouaboula, M.; Calandra, B.; Portier, M.; Shire, D.; Brelière, J. C.; Le Fur, G. L. SR 144528, the First Potent and Selective Antagonist of the CB_2 Cannabinoid Receptor. *J. Pharmacol. Exp. Ther.* **1998**, *284*, 644–650.

(32) Iwamura, H.; Suzuki, H.; Ueda, Y.; Kaya, T.; Inaba, T. In Vitro and in Vivo Pharmacological Characterization of JTE-907, a Novel Selective Ligand for Cannabinoid CB_2 Receptor. *J. Pharmacol. Exp. Ther.* **2001**, *296*, 420–425.

(33) Lavey, B. J.; Kozlowski, J. A.; Hipkin, R. W.; Gonsiorek, W.; Lundell, D. J.; Piwinski, J. J.; Narula, S.; Lunn, C. A. Triaryl Bis-Sulfones as a New Class of Cannabinoid CB_2 Receptor Inhibitors: Identification of a Lead and Initial SAR Studies. *Bioorg. Med. Chem. Lett.* **2005**, *15*, 783–786.

(34) Shankar, B. B.; Lavey, B. J.; Zhou, G.; Spitler, J. A.; Tong, L.; Rizvi, R.; Yang, D. Y.; Wolin, R.; Kozlowski, J. A.; Shih, N. Y.; Wu, J.; Hipkin, R. W.; Gonsiorek, W.; Lunn, C. A. Triaryl Bis-sulfones as Cannabinoid-2 Receptor Ligands: SAR Studies. *Bioorg. Med. Chem. Lett.* **2005**, *15*, 4417–4420.

(35) Lavey, B. J.; Kozlowski, J. A.; Shankar, B. B.; Spitler, J. M.; Zhou, G.; Yang, D. Y.; Shu, Y.; Wong, M. K.; Wong, S. C.; Shih, N. Y.; Wu, J.; McCombie, S. W.; Rizvi, R.; Wolin, R. L.; Lunn, C. A. Optimization of Triaryl Bis-sulfones as Cannabinoid-2 Receptor Ligands. *Bioorg. Med. Chem. Lett.* **2007**, *17*, 3760–3764.

(36) Lunn, C. A.; Fine, J. S.; Rojas-Triana, A.; Jackson, J. V.; Fan, X.; Kung, T. T.; Gonsiorek, W.; Schwarz, M. A.; Lavey, B.; Kozlowski, J. A.; Narula, S. K.; Lundell, D. J.; Hipkin, R. W.; Bober, L. A. A Novel Cannabinoid Peripheral Cannabinoid Receptor-Selective Inverse Agonist Blocks Leukocyte Recruitment in Vivo. *J. Pharmacol. Exp. Ther.* **2006**, *316*, 780–788.

(37) Idris, A. I.; van 't Hof, R. J.; Greig, I. R.; Ridge, S. A.; Baker, D.; Ross, R. A.; Ralston, S. H. Regulation of Bone Mass, Bone Loss and Osteoclast Activity by Cannabinoid Receptors. *Nature Med.* **2005**, *11*, 774–779.

(38) Idris, A. I.; Greig, I. R.; Bassonga-Landao, E.; Ralston, S. H.; van 't Hof, R. J. Identification of Novel Biphenyl Carboxylic Acid Derivatives as Novel Antiresorptive Agents That Do Not Impair Parathyroid Hormone-Induced Bone Bormation. *Endocrinology* **2009**, *150*, 5–13.

(39) Bab, I.; Ofek, O.; Tam, J.; Rehnelt, J.; Zimmer, A. Endocannabinoids and the Regulation of Bone Metabolism. *J. Neuroendocrinol.* **2008**, *20*, 69–74.

(40) Stern, E.; Muccioli, G. G.; Millet, R.; Goossens, J. F.; Farce, A.; Chavatte, P.; Poupaert, J. H.; Lambert, D. M.; Depreux, P.; Hénichart, J. P. Novel 4-Oxo-1,4-dihydroquinoline-3-carboxamide Derivatives as New CB_2 Cannabinoid Receptors Agonists: Synthesis, Pharmacological Properties and Molecular Modeling. *J. Med. Chem.* **2006**, *49*, 70–79.

(41) Stern, E.; Muccioli, G. G.; Bosier, B.; Hamtiaux, L.; Millet, R.; Poupaert, J. H.; Hénichart, J. P.; Depreux, P.; Goossens, J. F.;

Lambert, D. M. Pharmacomodulations Around the 4-Oxo-1,4-dihydroquinoline-3-carboxamides, a Class of Potent CB_2-Selective Cannabinoid Receptor Ligands: Consequences in Receptor Affinity and Functionality. *J. Med. Chem.* **2007**, *50*, 5471–5484.
(42) Kilbourn, E. E.; Seidel, M. C. Synthesis of *N*-Alkyl-3-carboxy-4-pyridones. *J. Org. Chem.* **1972**, *37*, 1145–1148.
(43) Li, Q.; Claiborne, A.; Li, T.; Hasvold, L.; Stoll, V. S.; Muchmore, S.; Jakob, C. G.; Gu, W.; Cohen, J.; Hutchins, C.; Frost, D.; Rosenberg, S. H.; Sham, H. L. Design, Synthesis, and Activity of 4-Quinolone and Pyridone Compounds as Nonthiol-Containing Farnesyltransferase Inhibitors. *Bioorg. Med. Chem. Lett.* **2004**, *14*, 5367–5370.
(44) McCombie, S. W.; Metz, W. A.; Nazareno, D.; Shankar, B. B.; Tagat, J. Generation and in Situ Acylation of Enaminone Anions: a Convenient Synthesis of 3-Carbethoxy-4(*1H*)-pyridinones and 4-pyrones and Related Compounds. *J. Org. Chem.* **1991**, *56*, 4963–4967.
(45) Govaerts, S. J.; Hermans, E.; Lambert, D. M. Comparison of Cannabinoid Ligands Affinities and Efficacies in Murine Tissues and in Transfected Cells Expressing Human Recombinant Cannabinoid Receptors. *Eur. J. Pharm. Sci.* **2004**, *23*, 233–243.
(46) Govaerts, S. J.; Muccioli, G. G.; Hermans, E.; Lambert, D. M. Characterization of the Pharmacology of Imidazolidinedione Derivatives at Cannabinoid CB_1 and CB_2 Receptors. *Eur. J. Pharmacol.* **2004**, *495*, 43–53.
(47) Muccioli, G. G.; Wouters, J.; Charlier, C.; Scriba, G. K.; Pizza, T.; Di Pace, P.; De Martino, P.; Poppitz, W.; Poupaert, J. H.; Lambert, D. M. Synthesis and Activity of 1,3,5-Triphenylimidazolidine-2,4-diones and 1,3,5-Triphenyl-2-thioxoimidazolidin-4-ones: Characterization of New CB_1 Cannabinoid Receptor Inverse Agonists/Antagonists. *J. Med. Chem.* **2006**, *49*, 872–882.
(48) Cherezov, V.; Rosenbaum, D. M; Hanson, M. A; Rasmussen, S. G.; Thian, F. S.; Kobilka, T. S.; Choi, H. J.; Kuhn, P.; Weis, W. I.; Kobilka, B. K.; Stevens, R. C. High-Resolution Crystal Structure of an Engineered Human Beta2-Adrenergic G Protein-Coupled Receptor. *Science* **2007**, *318*, 1258–1265.
(49) Rosenbaum, D. M.; Cherezov, V.; Hanson, M. A.; Rasmussen, S. G.; Thian, F. S.; Kobilka, T. S.; Choi, H. J.; Yao, X. J.; Weis, W. I.; Stevens, R. C.; Kobilka, B. K. GPCR Engineering Yields High-Resolution Structural Insights Into Beta2-Adrenergic Receptor Function. *Science* **2007**, *318*, 1266–1273.
(50) Rasmussen, S. G.; Choi, H. J.; Rosenbaum, D. M.; Kobilka, T. S.; Thian, F. S.; Edwards, P. C.; Burghammer, M.; Ratnala, V. R.; Sanishvili, R.; Fischetti, R. F.; Schertler, G. F.; Weis, W. I.; Kobilka, B. K. Crystal Structure of the Human Beta2 Adrenergic G-Protein-Coupled Receptor. *Nature* **2007**, *450*, 383–387.
(51) Kenakin, T. Inverse, Protean, and Ligand-Selective Agonism: Matters of Receptor Conformation. *FASEB J.* **2001**, *15*, 598–611.
(52) Lin, S. W.; Sakmar, T. P. Specific Tryptophan UV-Absorbance Changes Are Probes of the Transition of Rhodopsin to its Active State. *Biochemistry* **1996**, *35*, 11149–11159.
(53) Park, J. H.; Scheerer, P.; Hofmann, K. P.; Choe, H. W.; Ernst, O. P. Crystal Structure of the Ligand-Free G-Protein-Coupled Receptor Opsin. *Nature* **2008**, *454*, 183–187.
(54) Scheerer, P.; Park, J. H.; Hildebrand, P. W.; Kim, Y. J.; Krauss, N.; Choe, H. W.; Hofmann, K. P.; Ernst, O. P. Crystal Structure of Opsin in its G-Protein-Interacting Conformation. *Nature* **2008**, *455*, 497–502.
(55) Shi, L.; Liapakis, G.; Xu, R.; Guarnieri, F.; Ballesteros, J. A.; Javitch, J. A. Beta2 Adrenergic Receptor Activation. Modulation of the Proline Kink in Transmembrane 6 by a Rotamer Toggle Switch. *J. Biol. Chem.* **2002**, *277*, 40989–40996.
(56) McAllister, S. D.; Hurst, D. P.; Barnett-Norris, J.; Lynch, D.; Reggion, P. H.; Abood, M. E. Structural Mimicry in Class A G Protein-Coupled Receptor Rotamer Toggle Switches: The Importance of the F3.36(201)/W6.48(357) Interaction in Cannabinoid CB1 Receptor Activation. *J. Biol. Chem.* **2004**, *279*, 48024–48037.
(57) Muccioli, G. G.; Martin, D.; Scriba, G. K.; Poppitz, W.; Poupaert, J. H.; Wouters, J.; Lambert, D. M. Substituted 5,5′-Diphenyl-2-thioxoimidazolidin-4-one as CB_1 Cannabinoid Receptor Ligands: Synthesis and Pharmacological Evaluation. *J. Med. Chem.* **2005**, *48*, 2509–2517.
(58) Gouldson, P.; Calandra, B.; Legoux, P.; Kernéis, A.; Rinaldi-Carmona, M.; Barth, F.; Le Fur, G.; Ferrara, P.; Shire, D. Mutational Analysis and Molecular Modelling of the Antagonist SR 144528 Binding Site on the Human Cannabinoid CB_2 Receptor. *Eur. J. Pharmacol.* **2000**, *401*, 17–25.
(59) Xie, X. Q.; Chen, J. Z.; Billings, E. M. 3D Structural Model of the G-Protein-Coupled Cannabinoid CB_2 Receptor. *Proteins* **2003**, *53*, 307–319.
(60) Chen, J. Z.; Wang, J.; Xie, X. Q. GPCR Structure-Based Virtual Screening Approach for CB_2 Antagonist Search. *J. Chem. Inf. Model.* **2007**, *47*, 1626–1637.
(61) Sali, A.; Potterton, L.; Yuan, F.; van Vlijmen, H.; Karplus, M. Evaluation of Comparative Protein Modeling by MODELLER. *Proteins* **1995**, *23*, 318–326.
(62) Thompson, J. D.; Higgins, D. G.; Gibson, T. J. CLUSTAL W: Improving the Sensitivity of Progressive Multiple Sequence Alignment Through Sequence Weighting, Position-Specific Gap Penalties and Weight Matrix Choice. *Nucleic Acids Res.* **1994**, *22*, 4673–4680.
(63) Zhao, M. M.; Hwa, J; Perez, D. M. Identification of Critical Extracellular Loop Residues Involved in Alpha 1-Adrenergic Receptor Subtype-Selective Antagonist Binding. *Mol. Pharmacol.* **1996**, *50*, 1118–1126.
(64) Wurch, T.; Pauwels, P. J. Coupling of Canine Serotonin 5-HT(1B) and 5-HT(1D) Receptor Subtypes to the Formation of Inositol Phosphates by Dual Interactions with Endogenous G(i/o) and Recombinant G(alpha15) Proteins. *J. Neurochem.* **2000**, *75*, 1180–1189.
(65) Klco, J. M.; Wiegand, C. B.; Narzinski, K.; Baranski, T. J. Essential Role for the Second Extracellular Loop in C5a Receptor Activation. *Nature Struct. Mol. Biol.* **2005**, *12*, 320–326.
(66) Brooks, B. R.; Bruccoleri, R. E.; Olafson, B. D.; States, D. J.; Swaminathan, S.; Karplus, M. CHARMM: A Program for Macromolecular Energy Minimization and Dynamics Calculations. *J. Comput. Chem.* **1983**, *4*, 187–217.
(67) Jones, G.; Willett, P.; Glen, R. C.; Leach, A. R.; Taylor, R. Development and Validation of a Genetic Algorithm for Flexible Docking. *J. Mol. Biol.* **1997**, *267*, 727–748.